2.

Response of Simple Structures to Earthquake Ground Motions

2.1 INTRODUCTION

The main purpose of response analysis in earthquake engineering is the estimation of earthquake induced forces and deformations in structures under the action of earthquake ground motions. To this end, our approach will start with developing response analysis procedures for the simplest dynamic system, called the single degree of freedom system. These procedures are then extended to more complicated systems in the following chapters.

We will introduce the definition of a single degree of freedom system in this chapter first, and then derive the equations of motion governing its free vibration response (simple harmonic motion) and forced vibration response. Earthquake ground excitations lead to special forms of forced vibration response.

Single Degree of Freedom (SDOF) System:

The deformed shape of the system at any instant can be represented in terms of a single dynamic coordinate *u(t),* called the *single degree of freedom*. Single degree of freedom systems can be either "ideal SDOF systems", or "idealized SDOF systems".

Ideal SDOF Systems: Lumped Mass and Stiffness

The entire mass and stiffness of the system is lumped at a point where the dynamic coordinate *u(t)* is defined. The car in Fig. 2.1.a with mass *m* connected to a fixed end with a spring with stiffness *k*, which is free to move on rollers only in the lateral direction is a typical ideal SDOF system. An inverted pendulum type of structure where the lumped mass *m* is connected to the fixed base with a massless cantilever column is also an ideal SDOF system (Fig. 2.1.b). In this case the spring stiffness is identical to the lateral stiffness of the cantilever column, i.e. $k=3EI/L^3$. The motion of the mass and the elastic force which develops in the spring at any time *t* can be represented by the dynamic displacement *u(t)*, which is the single

degree of freedom in both systems. On the other hand, a pendulum where the mass m connected with a chord of length l that swings about the fixed end of the chord in the gravity field g is another example of an ideal SDOF system (Fig. 2.1.c). In this case the degree of freedom is the angle of rotation θ.

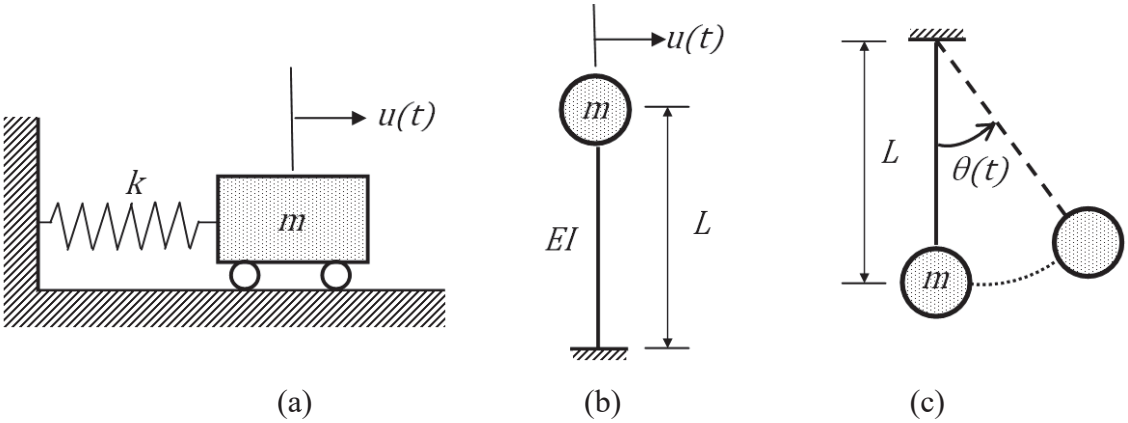

Figure 2.1. Ideal SDOF systems: (a) a car on rollers, (b) an inverted pendulum structure, (c) a pendulum swinging in the gravity field.

Idealized SDOF Systems: Distributed Mass

More complicated dynamic systems with distributed mass and stiffness can also be idealized as SDOF systems. Let's consider a cantilever column and a simple multistory frame in Fig. 2.2 where the lateral deformation shapes exhibit variation along the height during motion. Both systems can be defined as idealized SDOF systems if the lateral dynamic deformation distribution $u(x, t)$ along height x can be expressed as $u(x,t) = \phi(x) \cdot \bar{u}(t)$ where $\phi(x)$ is the normalized deformation profile, i.e. $\phi(L) = 1$. Lateral displacement $\bar{u}(t)$ at the top is the *single degree of freedom*. Note that $\phi(x)$ is assumed to be constant and not changing with time. This is not exactly correct, but practically acceptable. This assumption is valid for simple structural systems. For example, $\phi(x)=(x/L)^2$ is an acceptable normalized deformation shape for both SDOF systems in Fig. 2.2 since it satisfies the boundary conditions $u(0)=0$ and $u'(0)=0$ at $x=0$.

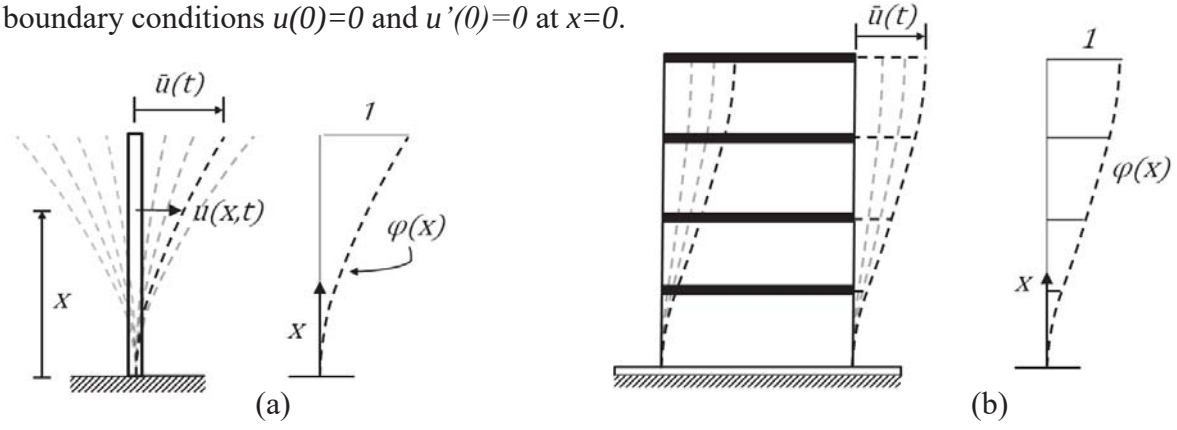

Figure 2.2. Idealized SDOF systems: (a) cantilever column, (b) multistory frame.

2.2 EQUATION OF MOTION: DIRECT EQUILIBRIUM

Consider two ideal SDOF systems in Fig. 2.3 with a mass, spring and damper. Damper is the only difference between Figs. 2.2 and 2.3, which represents internal friction in the actual mechanical system that is idealized as a SDOF system. Internal friction develops in deforming mechanical systems such as shown in Fig. 2.2 due to rubbing of the molecules with respect to each other during dynamic deformations. Internal friction leads to energy loss in a vibrating system.

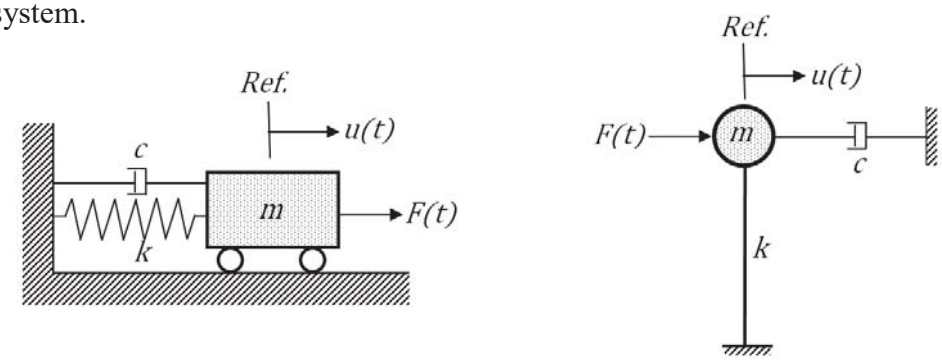

Figure 2.3. Ideal SDOF systems with mass *m*, stiffness *k* and damping *c*.

When the mass moves by a positive displacement $u(t)$ with a positive velocity $\dot{u}(t)$ under an external force $F(t)$, the spring develops a resisting force which is equal to $k \cdot u(t)$, and the damper develops a resisting force which equals $c \cdot \dot{u}(t)$, both in the opposite directions. Free body and kinetic diagrams of the masses in both SDOF systems are shown in Fig. 2.4.

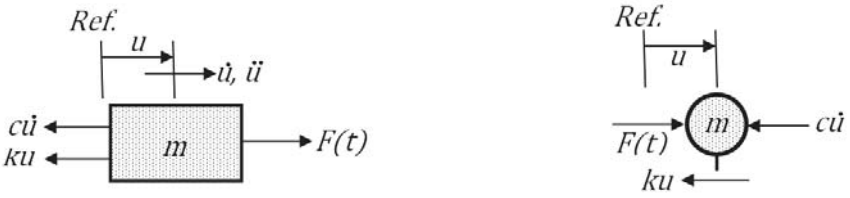

Figure 2.4. Free body diagrams of the masses when they displace by $u(t)$ and moving with a velocity of $\dot{u}(t)$ and an acceleration of $\ddot{u}(t)$ at time t

Applying Newton's second law of motion $\Sigma \underline{F} = m\underline{a}$ for dynamic equilibrium of the mass in the lateral direction leads to

$$F(t) - ku - c\dot{u} = m\ddot{u} \tag{2.1}$$

or

$$m\ddot{u} + c\dot{u} + ku = F(t) \tag{2.2}$$

This is a 2'nd order linear ordinary differential equation (ODE) with constant coefficients *m*, *c* and *k*.

2.3 EQUATION OF MOTION FOR BASE EXCITATION

The base of the inverted pendulum moves with the ground during an earthquake ground shaking with a ground displacement of $u_g(t)$ as shown in Fig. 2.5.a. There is no direct external force $F(t)$ acting on the mass when ground moves, but inertial force develops on the mass according to Newton's 2'nd law ($F=ma$) where a is the total acceleration of the mass ($a \equiv \ddot{u}^{total}$). It is the sum of ground acceleration and the acceleration of the mass relative to the ground.

$$\ddot{u}^{total} = \ddot{u}_g + \ddot{u} \tag{2.3}$$

Free body diagram of the mass is shown in Fig. 2.5.b. Then, according to Newton's 2'nd law, $\Sigma F = m\ddot{u}^{total}$ yields

$$-c\dot{u} - ku = m\ddot{u}^{total} \tag{2.4}$$

or

$$m(\ddot{u}_g + \ddot{u}) + c\dot{u} + ku = 0 \tag{2.5}$$

Transforming into the standard form of Eq.(2.2) leads to,

$$m\ddot{u} + c\dot{u} + ku = -m\ddot{u}_g(t) \equiv F_{eff}(t) \tag{2.6}$$

where $-m\ddot{u}_g(t)$ is considered as an effective force.

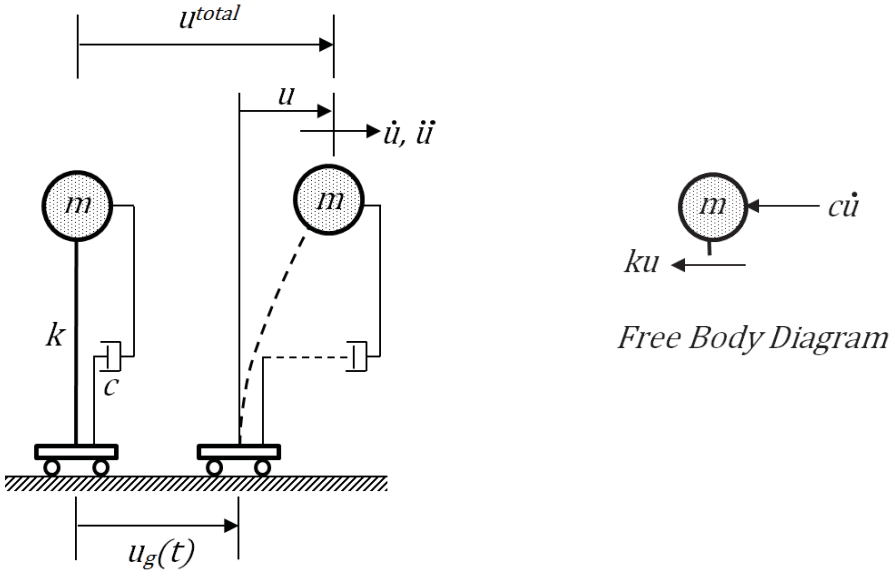

Figure 2.5. (a) An SDOF system under base excitation, (b) free body diagram of the mass when it displaces by $u(t)$, while moving with a velocity of $\dot{u}(t)$ and an acceleration of $\ddot{u}(t)$ at time t.

2.4 SOLUTION OF THE SDOF EQUATION OF MOTION

The solution of a 2'nd order ODE can be obtained in two parts:

$$u(t) = u_h(t) + u_p(t) \tag{2.7}$$

where u_h is the homogeneous solution and u_p is the particular solution. In vibration problem, u_h represents the free vibration response $(F = 0)$ and u_p represents the forced vibration response $(F \neq 0)$.

2.4.1 Free Vibration Response

The motion is imparted by the initial conditions at $t=0$: $u(0) = u_0$ (initial displacement) and $\dot{u}(0) = v_0$ (initial velocity). The equation of free vibration is given by

$$m\ddot{u} + c\dot{u} + ku = 0 \tag{2.8}$$

Dividing all terms by the mass m gives

$$\ddot{u} + \frac{c}{m}\dot{u} + \frac{k}{m}u = 0 \tag{2.9}$$

Let $\frac{c}{m} = 2\xi\omega_n$ and $\frac{k}{m} = \omega_n^2$. This is a simple replacement of the two coefficients $\frac{c}{m}$ and $\frac{k}{m}$ in terms of two new coefficients ξ and ω_n, which have distinct physical meanings. The dimensionless parameter ξ is the critical damping ratio, and ω_n is the natural frequency (rad/s). Vibration occurs only if $\xi < 1$. Then Eq. (2.9) can be written as,

$$\ddot{u} + 2\xi\omega_n\dot{u} + \omega_n^2 u = 0 \tag{2.10}$$

Undamped Free Vibration $(\xi = 0)$

When damping is zero, Eq. (2.10) reduces to

$$\ddot{u} + \omega_n^2 u = 0 \tag{2.11}$$

Eq. (2.11) represents simple harmonic motion. Only a harmonic function satisfies Eq. (2.11) with a harmonic frequency of ω_n. Its most general form is a combination of *sin* and *cos* functions with arbitrary amplitudes.

$$u(t) = A\sin\omega_n t + B\cos\omega_n t \tag{2.12}$$

A and *B* are determined by introducing the initial conditions $u(0) = u_0$ and $\dot{u}(0) = v_0$, leading to

$$u(t) = u_0 \cos \omega_n t + \frac{v_0}{\omega_n} \sin \omega_n t \tag{2.13}$$

Eq. (2.13) is shown graphically in Fig. 2.6.

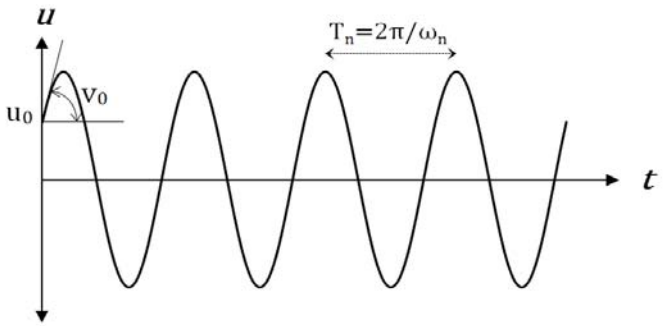

Figure 2.6. Undamped free vibrations of a SDOF system

Damped Free Vibration ($0<\xi<1$)

The presence of damping in free vibration imposes a decaying envelope on the undamped free vibration cycles in Fig. 2.6. Decay is exponential, and decay rate depends on $\omega_n t$, as given in Eq. (2.14).

$$u(t) = e^{-\xi\omega_n t}\left[u_0 \cos \omega_d t + \frac{v_0 + u_0 \xi \omega_n}{\omega_d} \sin \omega_d t\right] \tag{2.14}$$

The amplitude of harmonic vibration reduces exponentially at each cycle, and approaches zero asymptotically as shown in Fig. 2.7.

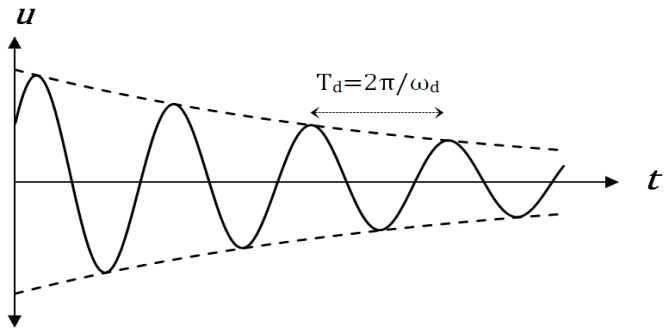

Figure 2.7. Free vibrations of a damped (under-damped) SDOF system

Note that the term in brackets in Eq. (2.14) is similar to Eq. (2.13) where ω_n is replaced by ω_d, which is the "damped" natural frequency given by Eq. (2.15).

$$\omega_d = \omega_n \sqrt{1 - \xi^2} \tag{2.15}$$

$\xi \leq 0.20$ for structural systems in general, hence $\omega_d \simeq \omega_n$. Typical viscous damping ratios that can be assigned to basic structural systems are given in Table 2.1.

Table 2.1. Typical damping ratios for basic structural systems

Structural type	**Damping ratio (%)**	
	<50% yield	**~ yield**
Steel (welded connections)	2-3	3-5
Reinforced concrete	3-5	5-10
Prestressed concrete	2-3	3-5
Masonry	5-10	10-20

Example 2.1. Consider the pendulum in Fig. (a) with mass *m* connected to a chord of length *L*, oscillating in the gravity field.

a) Determine its equation of motion.
b) Solve the equation of motion for small oscillations θ when the motion starts with an initial displacement θ_0.

a) At any $\theta(t)$, free body diagram of the mass is shown in Fig.(b), where *T* is the tension in the chord. Equation of motion in the t (tangential) direction can be written as

$$\Sigma F = ma_t$$

From Fig. (b),

$$-mg \sin\theta = ma_t \equiv mL\ddot{\theta}$$

Rearranging,

$$mL\ddot{\theta} + mg \sin\theta = 0 \qquad (Solution\ a) \tag{1}$$

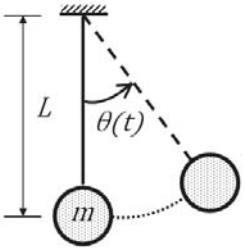

(a)

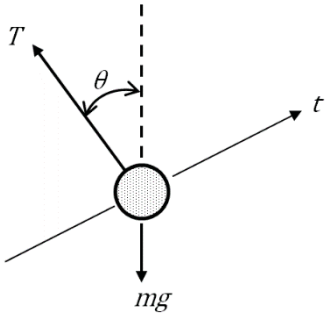

(b)

b) Eq. (1) is a 2nd order nonlinear ODE. Nonlinearity is due to the sin θ term. For small oscillations, sin $\theta \approx \theta$. Hence, the equation of motion becomes linear.

$$mL\,\ddot{\theta} + mg\,\theta = 0,$$

or

$$\ddot{\theta} + \frac{g}{L}\,\theta = 0.$$

With similitude to Eq. (2.11),

$$\omega_n^2 = \frac{g}{L} \;\; or \;\; T_n = 2\pi\sqrt{\frac{L}{g}}\,.$$

The solution from Eq. (2.12) is,

$$\theta(t) = A\sin\omega_n t + B\cos\omega_n t \tag{2}$$

Substituting $\theta\,(0) = \theta_0$ and $\dot{\theta}(0) = 0$ into Eq. (2), we obtain

$$\theta(t) = \theta_0\cos\sqrt{\frac{g}{L}}\,t \qquad (\textit{Solution b})$$

Example 2.2. Determine the natural frequency of vibration for the system shown in Fig. (a) where the bar AB is rigid and it has no mass.

The system in Fig. (a) is a SDOF system where the vertical displacement of end B can be employed as the DOF. The displacement variation of the SDOF system is always linear from A to B with a fixed shape as shown in Fig. (b).

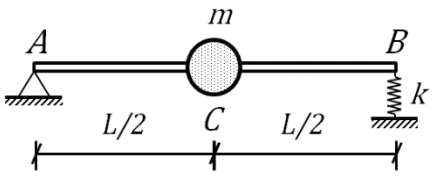

(a)

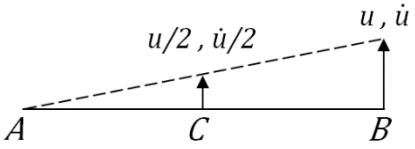

(b)

Since all forces are not directly acting on the mass, a direct formulation of the equation of motion is not possible. The conservation of energy principle provides a simpler approach.

$$T + U = Constant \tag{1}$$

where T is the kinetic energy and U is the potential energy at any time t, given by

$$T = \frac{1}{2}m\dot{u}^2 \;\; and \;\; U = \frac{1}{2}ku^2 \tag{2}$$

Here, we should consider from Fig. (b) that the velocity of the mass in terms of the DOF u is $\frac{\dot{u}}{2}$. Hence, $T = \frac{1}{2}\left(\frac{\dot{u}}{2}\right)^2$. Substituting into Eq. (1), and taking time derivative of both sides,

$$m\frac{\dot{u}}{2}\frac{\ddot{u}}{2} + ku\dot{u} = 0$$

or

$$\ddot{u} + 4\frac{k}{m} = 0$$

Accordingly,

$$\omega_n = 2\sqrt{\frac{k}{m}} \qquad (Solution)$$

Example 2.3. A single story, single bay portal frame is given below in Fig. (a).
a) Determine the equation of free vibration and the natural period of free vibration,
b) Determine the equation of motion under base excitation $\ddot{u}_g(t)$.

a) The portal frame is a SDOF system with the fixed deflection shape shown in Fig. (b). The lateral displacement u of the mass m at the roof is the degree of freedom. Free body diagram of the roof mass is given in Fig. (c).

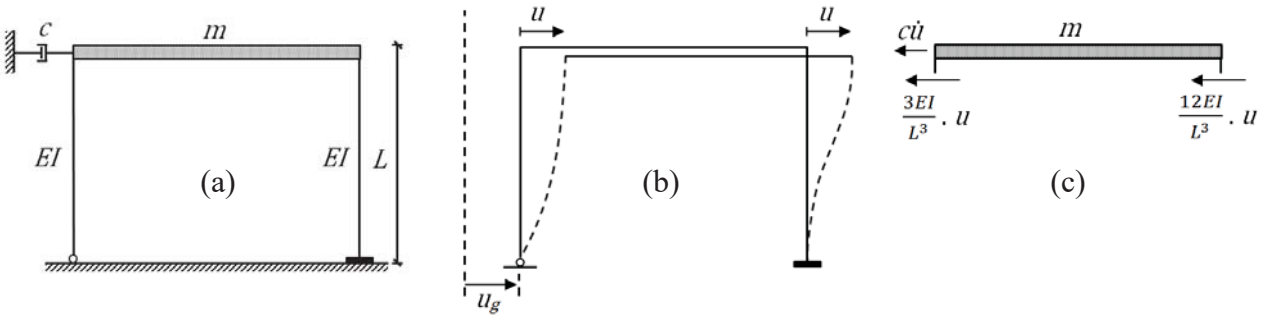

Applying Newton's second law of motion $\Sigma \underline{F} = m\underline{a}$ for dynamic equilibrium of the mass in the lateral direction leads to

$$-c\dot{u} - \frac{3EI}{L^3}u - \frac{12EI}{L^3}u = m\ddot{u} \qquad (1)$$

Rearranging,

$$m\ddot{u} + c\dot{u} + \frac{15EI}{L^3}u = 0$$

$\frac{15EI}{L^3}$ is the effective stiffness of the portal frame, and m is the mass. Accordingly,

$$\omega_n^2 = \frac{15EI}{mL^3} \quad and \quad T_n = 2\pi\sqrt{\frac{mL^3}{15EI}} \qquad (Solution\ a)$$

b) Eq. (1) can be written for base excitation as,

$$-c\dot{u} - \frac{15EI}{L^3}u = m\ddot{u}^{total} \equiv m(\ddot{u} + \ddot{u}_g)$$

or,

$$m\ddot{u} + c\dot{u} + \frac{15EI}{L^3}u = -m\ddot{u}_g \qquad (Solution\ b)$$

2.4.2 Forced Vibration Response: Harmonic Base Excitation

Harmonic excitation can either be applied as an external harmonic force, or an effective harmonic force due to a harmonic base excitation ($\ddot{u}_g(t) = a_0 \sin \bar{\omega} t$). Equation of motion under harmonic excitation can then be written as

$$m\ddot{u} + c\dot{u} + ku = F_0 \sin \bar{\omega}\, t \equiv -ma_0 \sin \bar{\omega} t \tag{2.16}$$

The homogeneous solution is identical to the damped free vibration response in Eq. (2.14), where vibration occurs at the free vibration frequency ω_d.

$$u_h = e^{-\xi\omega_n t} (A_1 \sin \omega_d t + A_2 \cos \omega_d t) \tag{2.17}$$

A_1 and A_2 are the arbitrary amplitudes that have to be determined from the initial conditions at t=0. However the initial conditions are imposed on the general (total) solution, not on the homogeneous solution alone.

The particular solution is assumed to be composed of *sin* and *cos* functions where vibration occurs at the forced vibration frequency $\bar{\omega}$.

$$u_p = G_1 \sin \bar{\omega} t + G_2 \cos \bar{\omega} t \tag{2.18}$$

The arbitrary harmonic amplitudes G_1 and G_2 are determined by using the method of undetermined coefficients for u_p.

$$G_1 = \frac{F_0}{k} \frac{1-\beta^2}{(1-\beta^2)^2+(2\xi\beta)^2} \; ; \; G_2 = \frac{F_0}{k} \frac{-2\,\xi\beta}{(1-\beta^2)^2+(2\xi\beta)^2} \; ; \; \beta = \frac{\bar{\omega}}{\omega_n} \tag{2.19}$$

General Solution

The general solution is the combination of homogeneous and particular solutions from Eqs. (2.17) and (2.18), respectively. Substituting G_1 and G_2 from Eq. (2.19) into Eq. (2.18), simplifying and collecting into $u(t)=u_h(t)+u_p(t)$, we obtain

$$u(t) = e^{-\xi\omega_n t} (A_1 \sin\omega_d t + A_2 \cos \omega_d t) + \frac{F_0}{k} \frac{(1-\beta^2) \sin \bar{\omega} t - 2\xi\beta \cos \bar{\omega} t}{(1-\beta^2)^2 + (2\xi\beta)^2} \tag{2.20}$$

A_1 and A_2 are determined from the initial conditions as indicated above.

In damped systems under harmonic excitation, u_h is called the transient and u_p is called the steady-state response since the transient part decays with time as shown in Fig. 2.7. If the transient part is ignored, then the remaining component u_p can also be expressed as

$$u = u_p = \rho \sin(\bar{\omega}t - \theta) \tag{2.21}$$

where

$$\rho = \frac{F_0/k}{[(1-\beta^2)^2 + (2\xi\beta)^2]^{1/2}} \quad , \quad \theta = \tan^{-1}\frac{2\xi\beta}{1-\beta^2} \tag{2.22}$$

Here, ρ is the amplitude, and θ is the phase lag (delay) between u_p and $F_0 \sin \bar{\omega}\, t$. It can be shown by expanding $\sin(\bar{\omega}t - \theta)$ that Eq. (2.21) with Eq. (2.22) is identical to the second (steady-state) term in Eq. (2.20). The variation of ρ with the frequency ratio β and the damping ratio ξ is plotted in Fig. 2.8, which is called the *frequency response function*. It can be observed that the response displacement amplitude amplifies as β approaches to unity whereas increase in damping ratio reduces the level of amplification.

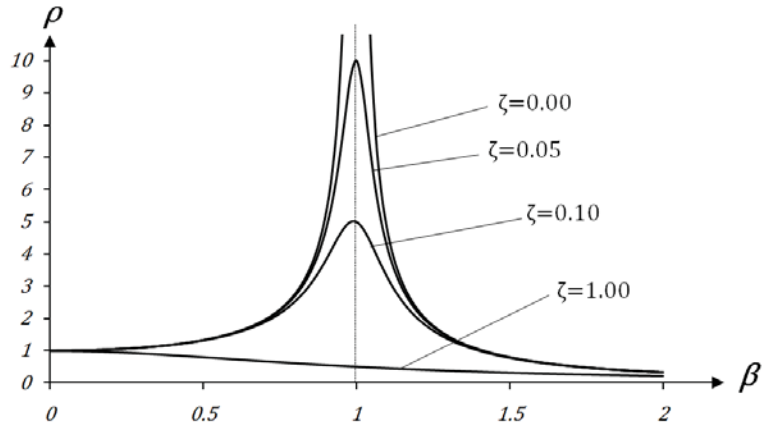

Figure 2.8. Frequency response function for damped systems under harmonic excitation

Resonance

When β=1, i.e. the forcing frequency $\bar{\omega}$ is equal to the natural frequency of vibration ω_n in Eq. (2.19), Eq. (2.18) reduces to

$$u(t) = \frac{F_0/k}{2\xi}\left(e^{-\xi\bar{\omega}t} - 1\right)\cos\bar{\omega}\, t \tag{2.23}$$

Eq. (2.23) is plotted in Fig. 2.9.a. The amplitude of displacement cycles increase at every cycle and asymptotically approach $\frac{F_0/k}{2\xi}$.

Meanwhile, if $\xi \rightarrow 0$, L'Hospital rule gives

$$u(t) = \frac{F_0/k}{2} \left(sin\, \bar{\omega} t - \omega t \cos \bar{\omega} t\right) \tag{2.24}$$

The second term in the parenthesis indicates a linear increase of displacement amplitude with time, without any bound. Eq. (2.24) is plotted in Fig. 2.9.b.

Eqs. (2.23) and (2.24) define a vibration phenomenon called the resonance. In mechanical systems, resonance causes very high displacements which usually lead to collapse.

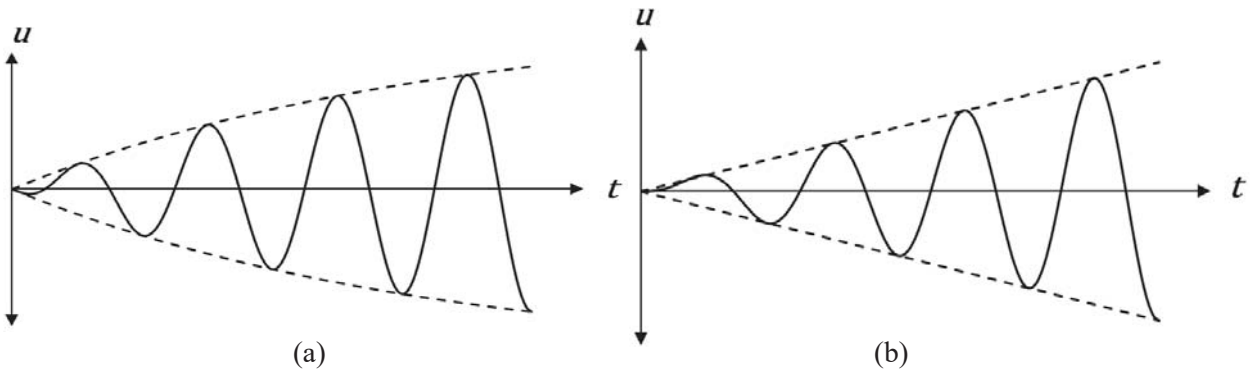

Figure 2.9. Resonance in (a) damped, (b) undamped SDOF systems under harmonic excitation

2.4.3 Forced Vibration Response: Earthquake Excitation

A SDOF system under earthquake ground acceleration is shown in Fig. 2.10. The excitation function *F(t)* or *(-mü$_g$ (t))* can rarely be expressed by an analytical function in the case of earthquake ground excitation. Ground acceleration *ü$_g$ (t)* is given numerically. Closed-form analytical solution similar to Eq. (2.20) is not possible. Then the solution is obtained by using numerical integration techniques. The most practical and also the most popular method is the *step-by-step direct integration* of the equation of motion (Newmark, 1956).

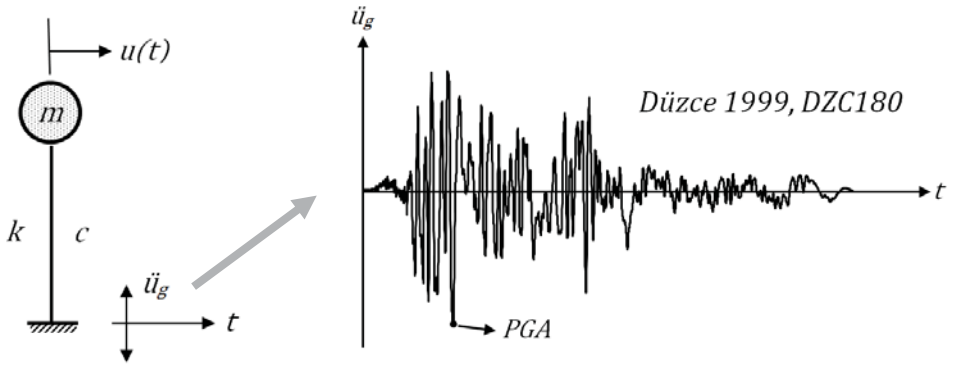

Figure 2.10. An SDOF system under earthquake excitation

Numerical Evaluation of Dynamic Response

Consider the equation of motion of a SDOF system at time $t = t_i$ and $t = t_{i+1} \equiv t_i + \Delta t$ where Δt is small.

$$m\ddot{u}_i + c\dot{u}_i + ku_i = F_i \tag{2.25.a}$$

$$m\ddot{u}_{i+1} + c\ddot{u}_{i+1} + ku_{i+1} = F_{i+1} \tag{2.25.b}$$

Subtracting (2.25.a) from (2.25.b) gives,

$$m(\ddot{u}_{i+1} - \ddot{u}_i) + c(\dot{u}_{i+1} - \dot{u}_i) + k(u_{i+1} - u_i) = F_{i+1} - F_i \tag{2.26}$$

or

$$m\Delta\ddot{u}_i + c\Delta\dot{u}_i + k\Delta u_i = \Delta F_i \tag{2.27}$$

where

$$\Delta(\cdot)_i = (\cdot)_{i+1} - (\cdot)_i \tag{2.28}$$

Eq. (2.27) contains three unknowns $(\Delta u_i\,,\ \Delta\dot{u}_i\,,\ \Delta\ddot{u}_i)$. Therefore it is indeterminate. However, we may impose two kinematical relations between these three response parameters, such as $(d\dot{u} = \ddot{u}dt)$ and $(du = \dot{u}dt)$. This can be achieved by assuming a variation of acceleration $\ddot{u}(t)$ over Δt, then integrating twice to calculate $\dot{u}(t)$ and $u(t)$ within Δt. We assume that $\ddot{u}_i\,,\ \dot{u}_i$ and u_i at the beginning of the time step are known from the previous step.

Two common assumption can be made on the variation of $\ddot{u}(t)$ over Δt : constant average acceleration and linear acceleration variation.

Constant Average Acceleration

Consider the variation of acceleration $\ddot{u}(t)$ over a time step Δt shown in Fig. 2.11. This actual variation can be estimated by an approximate, constant average acceleration variation given in Eq. (2.29).

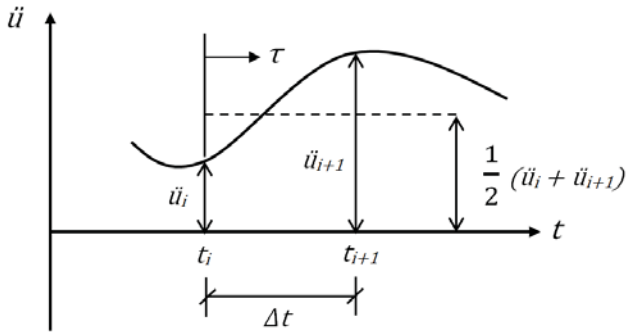

Fig. 2.11. Actual and estimated acceleration variations over a time step Δt.

$$\ddot{u}(\tau) = \frac{1}{2}\,(\ddot{u}_{\,i} + \ddot{u}_{i+1})\,; \qquad 0 < \tau < \Delta t \tag{2.29}$$

It should be noted here that the actual variation of acceleration on the left hand side of Eq. (2.29) is not known, and hence $\ddot{u}_{i+1}$ on the right hand side is also an unknown. This is merely a transfer of unknown from a function to a discrete value by the assumption of constant average acceleration variation.

We can integrate constant acceleration variation given in Eq. (2.29) twice, in order to obtain the variations of velocity and displacement over the time step Δt, respectively. This process is schematized in Fig. 2.12.

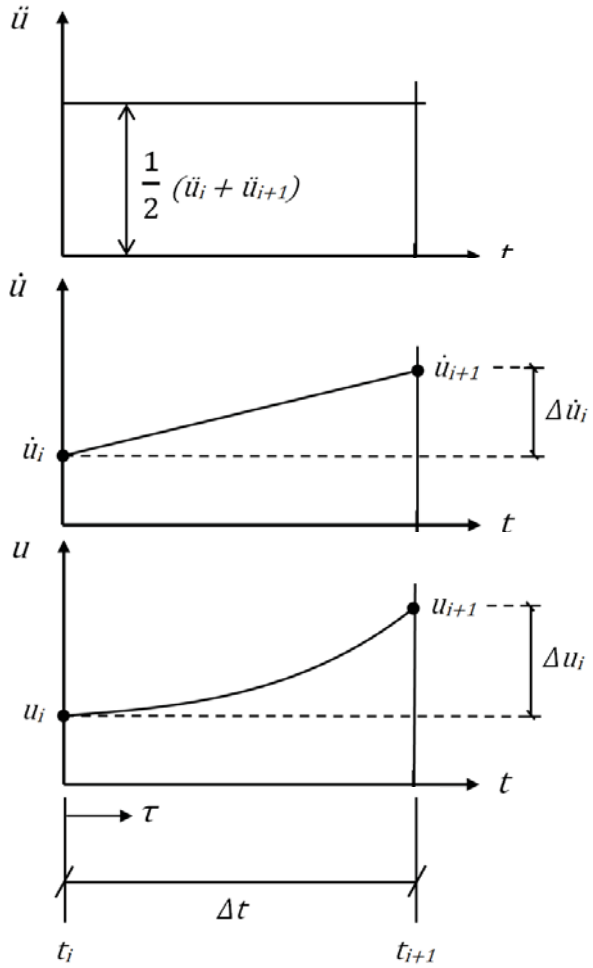

Fig. 2.12. Integration of constant average acceleration variation over the time step Δt

The first integration is from acceleration to velocity, i.e. the integration of $d\dot{u}=\ddot{u}d\tau$.

$$\int_{\dot{u}_i}^{\dot{u}} d\dot{u} = \int_{t_i}^{t} \ddot{u}d\tau \tag{2.30}$$

Substituting $\ddot{u}$ from Eq. (2.29) into Eq. (2.30) and integrating, we obtain

$$\dot{u}(\tau) = \dot{u}_i + \frac{\tau}{2}(\ddot{u}_i + \ddot{u}_{i+1}) \tag{2.31}$$

Eq. (2.31) can also be written for $\tau = t_{i+1}$ at the end of the time step which gives

$$\dot{u}_{i+1} = \dot{u}_i + \frac{\Delta t}{2}(\ddot{u}_i + \ddot{u}_{i+1}) \tag{2.32}$$

Then, substituting $\dot{u}$ from Eq. (2.31) into $du = \dot{u}d\tau$ and integrating over Δt,

$$\int_{u_i}^{u_{i+1}} du = \int_{t_i}^{t_i+\Delta t} \dot{u}d\tau \tag{2.33}$$

we obtain

$$u_{i+1} = u_i + \dot{u}_i \Delta t + \frac{\Delta t^2}{4}(\ddot{u}_i + \ddot{u}_{i+1}) \tag{2.34}$$

The terms u_{i+1}, $\dot{u}_{i+1}$ and $\ddot{u}_{i+1}$ at t_{i+1} in Eqs. (2.32) and (2.34) are the unknowns.

Let$(\ddot{u}_i + \ddot{u}_{i+1}) \equiv \ddot{u}_{i+1} - \ddot{u}_i + 2\ddot{u}_i \equiv \Delta\ddot{u}_i + 2\ddot{u}_i$. When this identity is substituted into Eqs. (2.32) and (2.34) and rearranged, two new equations are obtained:

$$\Delta\dot{u}_i = \frac{\Delta t}{2}(\Delta\ddot{u}_i + 2\ddot{u}_i) \tag{2.35}$$

$$\Delta u_i = \dot{u}_i \Delta t + \frac{\Delta t^2}{4}(\Delta\ddot{u}_i + 2\ddot{u}_i) \tag{2.36}$$

Δu_i, $\Delta\dot{u}_i$ and $\Delta\ddot{u}_i$ are the new three unknowns in Eqs. (2.35) and (2.36). Combining these equations with Eq. (2.27) forms a system of three coupled linear equations with three unknowns, and can be solved through elimination.

Let's rearrange (2.35) and (2.36) to express $\Delta\ddot{u}_i$ and $\Delta\dot{u}_i$ in terms of Δu_i. From Eq. (2.36),

$$\Delta\ddot{u}_i = \frac{4}{\Delta t^2}\Delta u_i - \frac{4}{\Delta t}\dot{u}_i - 2\ddot{u}_i \tag{2.37}$$

Substituting $\Delta\ddot{u}_i$ above into Eq. (2.35),

$$\Delta\dot{u}_i = \frac{2}{\Delta t}\Delta u_i - 2\dot{u}_i \tag{2.38}$$

Finally, substituting $\Delta\ddot{u}_i$ and $\Delta\dot{u}_i$ from Eqs. (2.37) and (2.38) into Eq. (2.27) and rearranging, we obtain

$$k_i^* \Delta u_i = \Delta F_i^* \tag{2.39}$$

where

$$k_i^* = k + \frac{2c}{\Delta t} + \frac{4m}{\Delta t^2} \tag{2.40}$$

is the instantaneous dynamic stiffness, and

$$\Delta F_i^* = \Delta F_i + \left(\frac{4m}{\Delta t} + 2c\right)\dot{u}_i + 2m\ddot{u}_i \tag{2.41}$$

is the effective dynamic incremental force. Note that $k_i^* = k^*$ in Eq. (2.40), i.e. dynamic stiffness does not change at each time step *i*.

The recursive solution starts at $i = 0$ with $u(0) = 0$ and $\dot{u}(0) = 0$ as the initial conditions. This procedure is unconditionally stable: Errors do not grow up with the recursion steps. However $\frac{\Delta t}{T_n} \leq 10$ is required for accuracy.

The step-by-step direct integration procedure described above is formulated as an algorithm below, which can be easily coded with conventional software (FORTRAN, MathLab, Excel, etc.).

Integration Algorithm

1. DEFINE $m, c, k, u(0) = 0, \dot{u}(0) = 0, F_i = F(t_i)$ and Δt
2. $\ddot{u}_0 = \frac{1}{m}(F_0 - c\dot{u}_0 - ku_0)$
3. CALCULATE k^* from Eq. (2.40)
4. $i = i + 1$
5. CALCULATE ΔF_i^* from Eq. (2.41)
6. $\Delta u_i = {}^{\Delta F_i^*}/_{k^*}$
7. CALCULATE $\Delta\dot{u}_i$ and $\Delta\ddot{u}_i$ from Eqs. (2.37) and (2.38)
8. $(\cdot)_{i+1} = (\cdot)_i + \Delta(\cdot)_i$ for $(\cdot) = u, \dot{u}, \ddot{u}$
9. GO TO *4*

Example 2.4. A linear elastic SDOF system is given with T_n = 1 s, m = 1 kg (unit), ξ = 5%, $u(0) = \dot{u}(0) = 0$ (initially at rest). Determine the displacement response, $u(t)$ under the base excitation $\ddot{u}_g(t)$ defined below. Use Δt = 0.1 second in calculations.

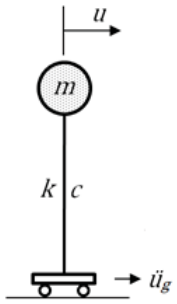

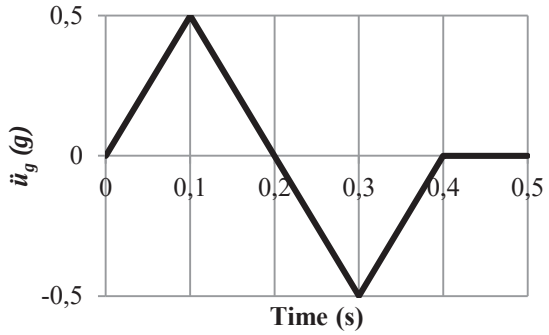

Solution

$\omega_n = \frac{2\pi}{T_n} = 6{,}28\ rad/s^2, \quad k = \omega_n{}^2 m = 39{,}478\ N/m, \quad c = 2\xi m\omega_n = 0{,}628\ N \cdot s/m$

$$\ddot{u}_0 = \frac{1}{m}\left[-m\ddot{u}_{g(0)} - c\dot{u}_0 - ku_0\right] = 0, \quad k^* = k + \frac{2c}{\Delta t} + \frac{4m}{\Delta t^2} = 452{,}045\ N/m$$

m	T_n (s)	ω_n (rad/s)	ξ	Δt (s)	c	k	u_0	$\dot{u}_0$	$\ddot{u}_0$	k^*
1	1	6,28	0,05	0,1	0,628	39,478	0	0	0	452,045

$$\Delta F_i^* = \Delta F_i + \left(\frac{4m}{\Delta t} + 2c\right)\dot{u}_i + 2m\ddot{u}_i \quad \text{where} \quad \Delta F_i = -m\left(\ddot{u}_{g(i+1)} - \ddot{u}_{g(i)}\right)$$

$\underline{i = 0}$: $\Delta F_0^* = -1 * (0{,}5 - 0) * 9{,}81 + \left[\left(\frac{4*1}{0{,}1}\right) + 2 * 0{,}628\right] * (0) + 2 * 1 * (0) = -4.905\ N$

i	t	u_i	$\dot{u}_i$	$\ddot{u}_i$	ΔF_i^*	Δu_i	$\Delta \dot{u}_i$	$\Delta \ddot{u}_i$	u_{i+1}	$\dot{u}_{i+1}$	$\ddot{u}_{i+1}$
0	0	0	0	0	-4,905	-0,0109	-0,2170	-4,3403	-0,0109	-0,2170	-4,3403
1	0,1	-0,0109	-0,2170	-4,3403	-12,729	-0,0282	-0,1291	6,0978	-0,0390	-0,3462	1,7575
2	0,2	-0,0390	-0,3462	1,7575	-5,861	-0,0130	0,4330	5,1448	-0,0520	0,0868	6,9023
3	0,3	-0,0520	0,0868	6,9023	12,482	0,0276	0,3786	-6,2330	-0,0244	0,4654	0,6693
4	0,4	-0,0244	0,4654	0,6693							

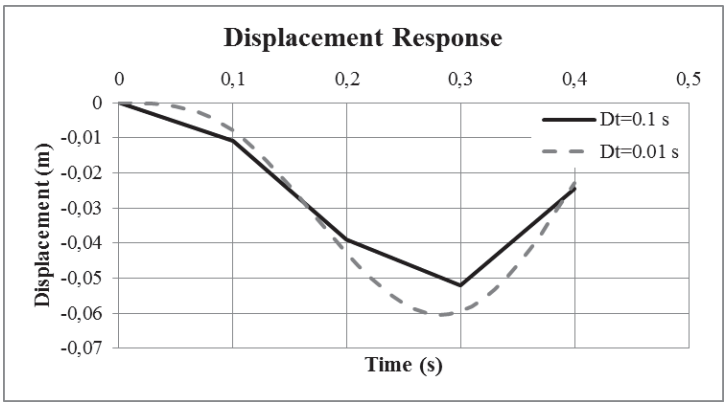

Note: Solution with Δt =0.01 seconds can be considered as exact.

2.5 EARTHQUAKE RESPONSE SPECTRA

Consider various SDOF systems with different T, but the same ξ, subjected to a ground excitation as shown in Fig. 2.13. Note that $T_1 < T_2 < T_3 < \cdots$ in Fig. 2.13.

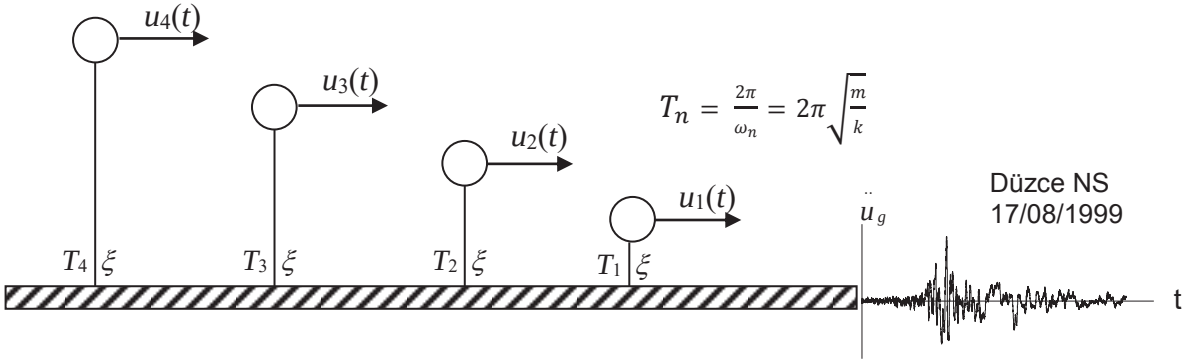

Fig. 2.13. Different SDOF systems under earthquake ground excitation

We can calculate the displacement response of each SDOF system *u(t)* by direct integration. Time variations *u(t)* and *ü(t)* of 5 percent damped SDOF systems with T_1=0.5 s, T_2=1.0 s and T_3=2.0 s under the NS component of 1999 Düzce ground motion are plotted in Fig. 2.14.

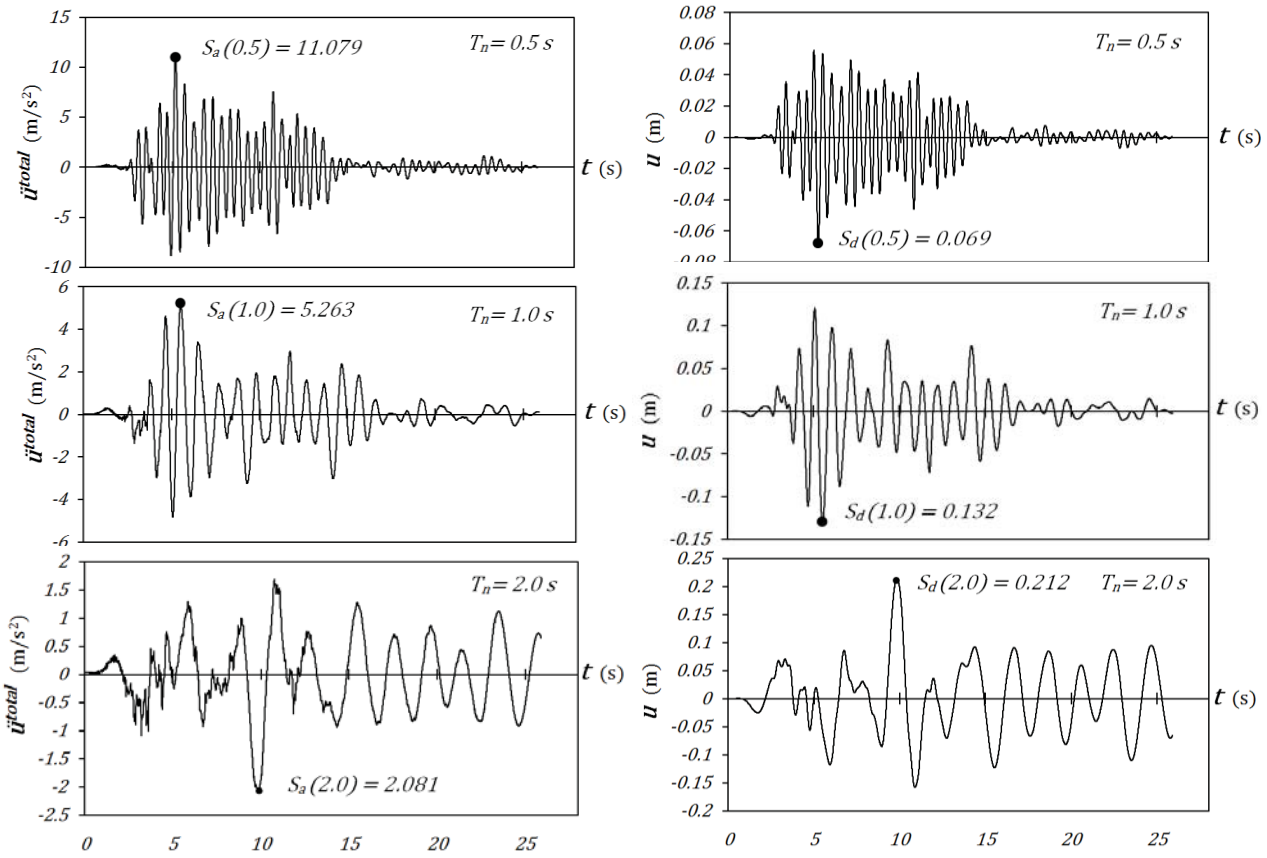

Fig. 2.14. Time variations of displacement and acceleration responses of several SDOF systems under the NS component of 1999 Düzce ground motion

We can select the peak displacement response from each *u(t)* function, and define this value as the spectral displacement S_d, where,

$$S_d = max\ |u(t)| \tag{2.42}$$

Since each *u(t)* is a function of T and ξ, S_d also varies with *T* and ξ. Hence,

$$S_d = S_d(T, \xi) \tag{2.43}$$

Similarly, spectral acceleration can be defined as the peak value of total acceleration

$$S_a = max\left|\ddot{u}(t) + \ddot{u}_g(t)\right| \tag{2.44}$$

where

$$S_a = S_a(T, \xi) \tag{2.45}$$

S_a and S_d values are marked on Fig. 2.14 for the response of each SDOF system.

Accordingly, S_d and S_a in Eqs. (2.43) and (2.45) can be plotted as functions of T and ξ. When this process is repeated for a set of damping ratios, a family of S_a and S_d curves are obtained. The family of these curves is called the *acceleration response spectra* and *displacement response spectra* of an earthquake ground motion, respectively. Acceleration and displacement response spectra of the NS component of 1999 Düzce ground motion are plotted in Fig. 2.15. The peak values indicated in Fig. 2.14 are also marked on Fig. 2.15.

The duration effect is almost lost in the spectral information since an earthquake response spectrum only considers the time when peak response occurs. This is practical for design, however a long duration ground motion may cause low cycle fatigue and consequent degradation. We cannot obtain such detailed information from a response spectrum.

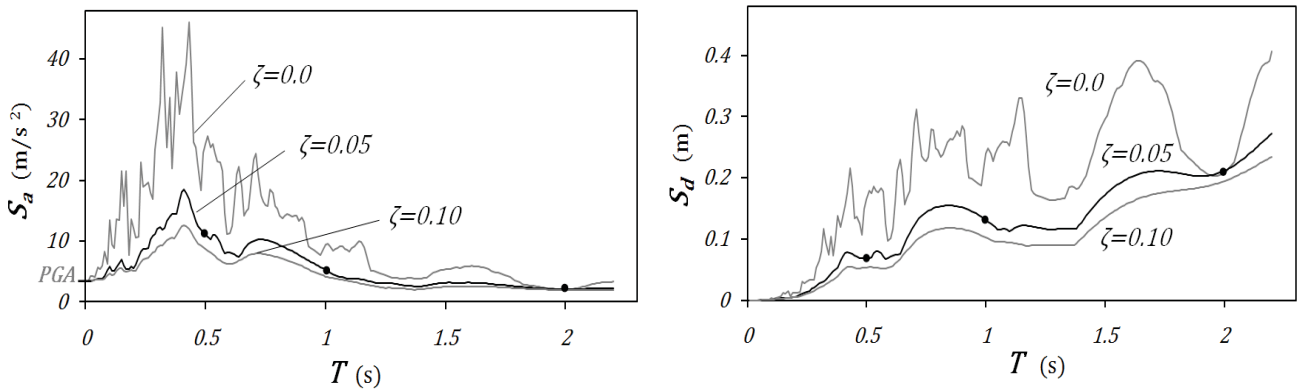

Fig. 2.15. Acceleration and displacement response spectra of the NS component of 1999 Düzce ground motion

It can be observed from Fig. 2.15 that when T=0, $S_a = \ddot{u}_{g,max}$ (PGA) and $S_d = 0$. On the other hand, when T approaches infinity, S_a approaches zero and S_d approaches $u_{g,max}$ (PGD). These limiting situations can be explained with the aid of Fig. 2.16.

T=0 is equivalent to $\omega_n = \infty$, i.e. the system is infinitely stiff. Then the spring does not deform (u=0, hence $S_d = 0$) and the motion of the mass becomes identical to the motion of ground. Accordingly, maximum acceleration of the mass becomes identical to the acceleration of the ground which makes their maximum values equal.

T approaches infinity when ω_n approaches zero. Hence the system becomes infinitely flexible. An infinitely flexible system has no stiffness and it cannot transmit any internal lateral force from the ground to the mass above. Ground moves while the mass stays stationary during the earthquake. The total displacement of the mass is zero ($u^{total} = u+u_g = 0$). Accordingly $|u|_{\max}=|u_g|_{max}$, or $S_d = PGD$. Similarly, the total acceleration of the mass is zero ($\ddot{u}^{total}=\ddot{u}+\ddot{u}_g=0$) which makes $S_a=0$ from Eq. (2.44).

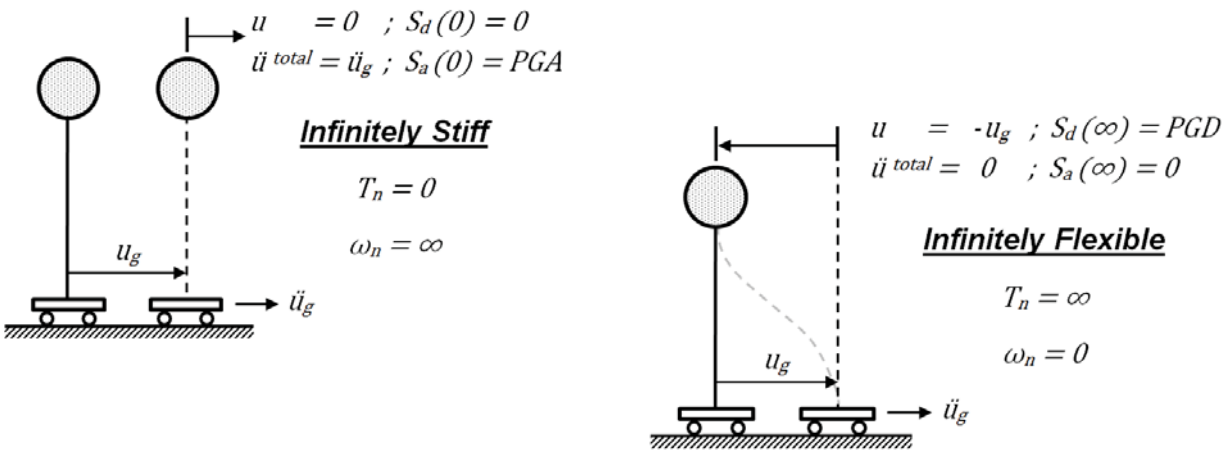

Fig. 2.16. Response of infinitely stiff and infinitely flexible SDOF systems to ground excitation

2.5.1 Pseudo Velocity and Pseudo Acceleration Response Spectrum

Pseudo spectral velocity PS_v and pseudo spectral acceleration PS_a can be directly obtained from S_d. Their definitions are given in Eqs. (2.46) and (2.48) below. PS_v and PS_a are very close to S_v and S_a respectively, for $\xi < 0.20$.

Pseudo Velocity

$$PS_v(T,\xi) = \omega_n . S_d = \frac{2\pi}{T_n} S_d(T,\xi) \tag{2.46}$$

$PS_v \approx S_v$ for $\xi < 0.20$. It is related to the maximum strain energy E_s stored in the SDOF system during the earthquake.

$$E_{s,max} = \frac{1}{2} k\ u_{max}^2 = \frac{1}{2} k\ S_d^2 = \frac{1}{2} k \left(\frac{PS_v}{\omega_n}\right)^2 = \frac{1}{2} m\ (PS_v)^2 \tag{2.47}$$

Pseudo Acceleration

$$PS_a(T,\xi) = \omega_n^2\, S_d = \left(\frac{2\pi}{T_n}\right)^2 S_d(T,\xi) \tag{2.48}$$

$PS_a \approx S_a$ for $\xi<0.20$. It is related to the maximum base shear force at the support of the SDOF system during the earthquake.

Lets consider an undamped SDOF system under a ground excitation $\ddot{u}_g$. Its equation of motion is,

$$m\left(\ddot{u} + \ddot{u}_g\right) + ku = 0 \tag{2.49}$$

Therefore,

$$m\left|\left(\ddot{u}+\ddot{u}_g\right)\right|_{max} = k|u|_{max} \tag{2.50}$$

Then,

$$mS_a = kS_d \quad \text{or} \quad S_a = \omega_n^2 S_d \tag{2.51}$$

for ξ=0. Comparison of Eqs. (2.48) and (2.51) indicates that PS_a=S_a when ξ=0.

The shear (restoring) force and base shear force which develop in a SDOF system during an earthquake ground excitation are shown in Fig. 2.17. Base shear force becomes maximum when the relative displacement is maximum, i.e.,

$$V_{b,max} = ku_{max} = k\,S_d = k\left(\frac{S_a}{\omega_n^2}\right) = m\,S_a \tag{2.52}$$

Now, let's consider a damped SDOF system. Eq. (2.52) is replaced by

$$V_{b,max} = ku_{max} = k\,S_d = k\left(\frac{PS_a}{\omega_n^2}\right) = m\,PS_a \tag{2.53}$$

Hence, the maximum base shear force in an undamped SDOF system can directly be obtained from PS_a through Newton's second law.

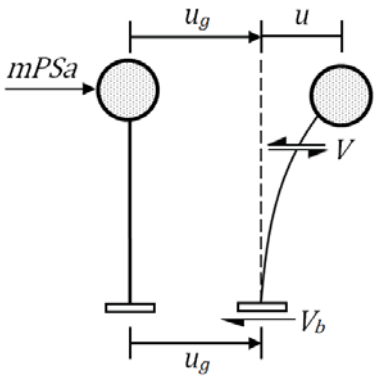

Fig. 2.17. Internal shear force and base shear force developing in an SDOF system under earthquake ground excitation

2.5.2 Practical Implementation of Earthquake Response Spectra

If S_d, PS_v and PS_a are available for an earthquake ground excitation, then we can easily obtain the maximum values of response displacement, strain energy, internal elastic force and base shear force of an SDOF system from these spectral charts. The only data we need for a SDOF system is its natural vibration period T_n and viscous damping ratio ξ.

The maximum base shear force in Eq. (2.53) can be formulated as follows:

$$V_{b,max} = m\,PS_a = mg\,\frac{PS_a}{g} = W.\frac{PS_a}{g} \tag{2.54}$$

where W is the weight in the gravity field. Then,

$$\frac{V_{b,max}}{W} = \frac{PS_a}{g} \tag{2.55}$$

The ratio of maximum base shear force to weight is called the *base shear coefficient*, which is a practical yet very important parameter in earthquake engineering analysis and design. It is denoted with *C*, and it can be obtained directly from PS_a.

$$C = \frac{V_{b,max}}{W} = \frac{PS_a}{g} \tag{2.56}$$

Example 2.5. Consider the portal frame in Example 2.3. The properties assigned are, column size: 0.40x0.50 m, E=250,000 kN/m^2, L=3m and m=25 tons. Determine the maximum displacement of the roof if the frame is subjected to the 1999 Düzce NS ground motion. Viscous damping ratio is 5 %.

The natural vibration period was defined in Example 2.3. When the numerical values given above are substituted, T_n =1.3 seconds is calculated. Then the spectral acceleration can be determined from Fig. (2.15) at T=1.3 seconds as S_a = 4 m/s^2.

The effective force acting at the roof mass is,

$$F_{eff} = mS_a = 25 \text{ tons x } 4 \text{ m/s}^2 = 100 \text{ kN}$$

The effective stiffness expression was also derived in Example 2.3. When the numerical values given above are substituted, k_{eff} = 578.7 kN/m is calculated. Finally,

$$u = \frac{F_{eff}}{k_{eff}} = 0.173 \text{ m} \qquad (Solution)$$

2.5.3 Normalization of Earthquake Response Spectra

Spectral acceleration shapes for different earthquake ground motions exhibit significant variations, as shown in Fig. 2.18.a for a suit of 10 ground motions. They are usually normalized by selecting a fixed damping ratio first, usually ξ = 0.05, then removing the effect of with peak ground acceleration $\ddot{u}_{g,max}$ (*PGA*) by dividing $S_a(T)$ with *PGA* for all *T*. The spectral acceleration shapes normalized with respect to *PGA* in Fig. 2.18.b. display less variation compared to the non-normalized spectra in Fig. 2.18.a.

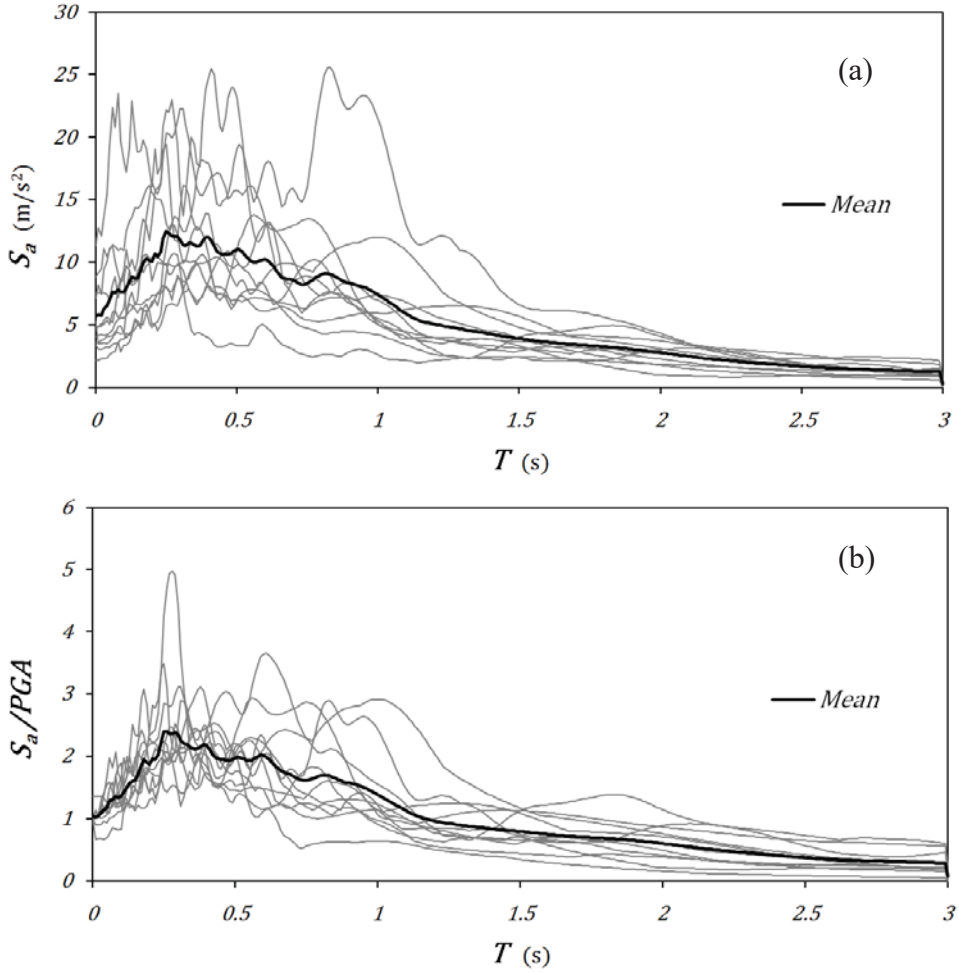

Fig. 2.18. (a) Acceleration response spectra of 10 ground motions, (b) acceleration response spectra of 10 ground motions normalized with respect to their peak ground accelerations.

It is possible to obtain statistical averages of $S_a(T)/PGA$ over period (Fig. 2.18.b). However, this is usually done first by grouping the ground motions with respect to the soil conditions of the recording stations (sites), then obtaining the mean values of $S_a(T)/PGA$ values over T. This exercise was first carried out by Seed et al. (1976) which indicate the effect of local soil conditions on the shape of mean acceleration spectra (Fig. 2.19). These shapes form the basis of earthquake design spectra defined for local soil conditions, which will be discussed in Chapter 4.

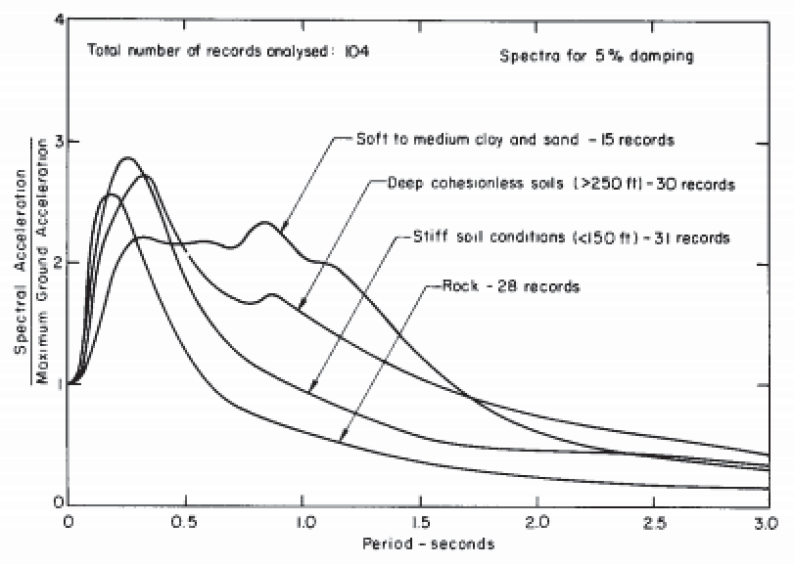

Fig. 2.19. (a) Mean normalized acceleration response spectra of ground motions classified with respect to local soil conditions *(Seed, H. B., Ugas, C. and Lysmer, J. (1976) , "Site-dependent spectra for earthquake-resistant design", Bull.Seism. Soc. Am. 66, No.1, 221-243*).

2.6 NONLINEAR SDOF SYSTEMS

The lateral forces which act on linear elastic structural systems under severe earthquake ground motions are usually very large. It can be observed from Fig. 2.18.a that the effective lateral forces ($m \cdot PS_a$) are at the order of the weight (mg) in the period range of 0.4-1.0 seconds. Fundamental vibration periods of most of the building structures fall into this period range. Designing structures for such high levels of lateral forces is not economical and feasible for a very seldom event such as a strong earthquake which may occur only with a small probability during its service life. The preferred approach in seismic design is to provide a lateral strength F_y that is less than the elastic strength demand F_e, however implement a plastic deformation capacity to the system such that it can deform beyond the linear elastic range during a strong ground motion.

When the yield displacement capacity of the lateral load resisting system is exceeded, the slope of the restoring force-deformation curve, or stiffness softens. A typical force-deformation path of a SDOF system subjected to a single cycle of large ground displacement is shown in Fig. 2.20. This type of nonlinear behavior is called *material nonlinearity* in mechanical systems because softening occurs due to the deterioration of material properties at large displacements, similar to the stress-strain behavior of steel and concrete materials. F_s is the restoring force (internal resistance), F_y is the yield force capacity and u_y is the yielding displacement in Fig. 2.20.

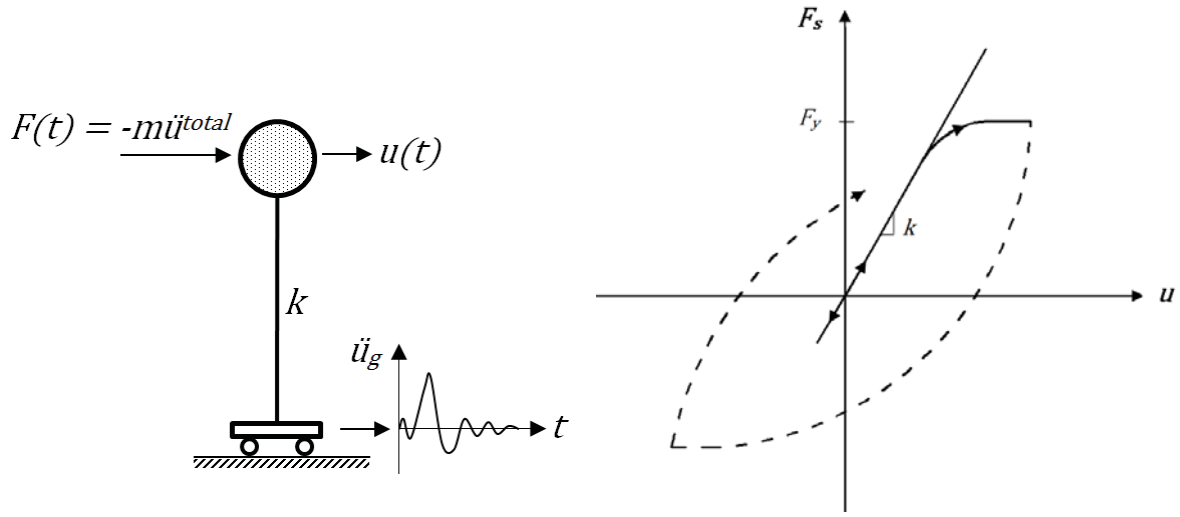

Fig. 2.20. Variation of internal force F_s with displacement u along a nonlinear force-deformation path.

2.6.1 Equation of Motion of a Nonlinear SDOF System

Equation of motion of a nonlinear SDOF system is also mathematically nonlinear.

$$m\ddot{u} + c\dot{u} + F_s(u) = -m\ddot{u}_g \tag{2.57}$$

The restoring force term F_s creates the nonlinearity in the equation of motion since $F_s(u)$ is a nonlinear function. In a linear system, F_s is equal to $k\,u$ which is a linear relationship between F_s and u whereas $F_s = F_s(u)$ in a nonlinear system which implies that the tangent stiffness k is not constant as in a linear system, but changes with the displacement u. The variation of F_s with u along a nonlinear force-deformation path is schematized in Fig. 2.20.

The equation of motion can be written in incremental form with the aid of Fig. 2.21.

$$m\Delta\ddot{u}_i + c\Delta\dot{u}_i + \Delta F_s\,(\Delta u)_i = -m\Delta\ddot{u}_{gi} \tag{2.58}$$

The incremental variation of restoring force F_s with u can be estimated with

$$\Delta F_{si} \approx k_i(u_i)\,\Delta u_i \tag{2.59}$$

where

$$F_{si+1} = F_{si} + \Delta F_{si} \quad \text{and} \quad u_{i+1} = u_i + \Delta u_i \tag{2.60}$$

and k_i is the tangent stiffness at u_i.

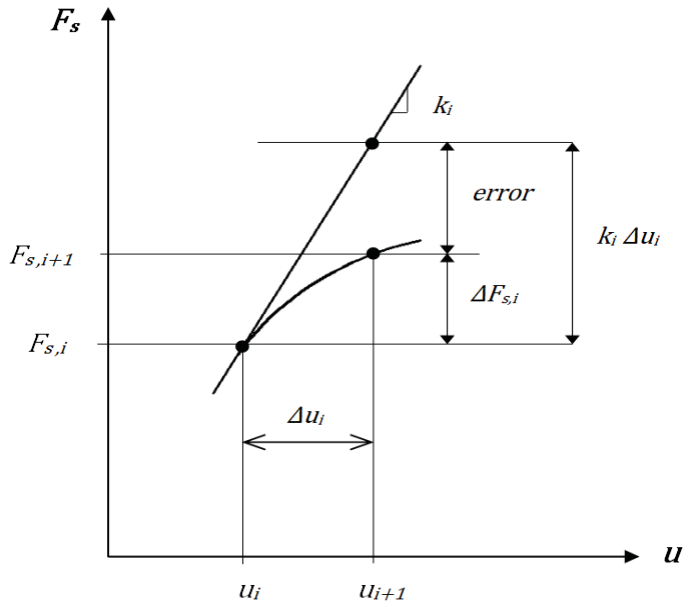

Fig. 2.21. Incremental variation of F_s and u.

Step-by-step direct integration algorithm developed for linear elastic systems in **2.4.3** can be applied to nonlinear systems if tangent stiffness k_i (u_i) is known and hence can be updated at each load step i. This requires a priori knowledge of the F_s (u) function, which is called the *hysteresis relationship*.

2.6.2 Nonlinear Force-Deformation Relations

Hysteresis relations are composed of a set of rules by which the variation of F_s is defined in terms of the variation history of u during the previous loading steps. This is called a *hysteresis model*. Two basic hysteresis models are employed in earthquake engineering: Elasto-plastic and stiffness degrading models. The elasto-plastic model is usually employed for representing the hysteretic flexural behavior of steel structures whereas the stiffness degrading model represents the hysteretic flexural behavior of concrete structures respectively, under loading reversals induced by an earthquake ground motion.

The set of rules which define elasto-plastic and stiffness degrading hysteretic behavior with strain hardening are shown in Fig. 2.22. F_y and u_y are the yield strength and yield displacement respectively, k is the initial elastic stiffness and αk is the strain hardening stiffness after yielding where α is usually less than 10 percent. When α=0, the system is elastic-perfectly plastic.

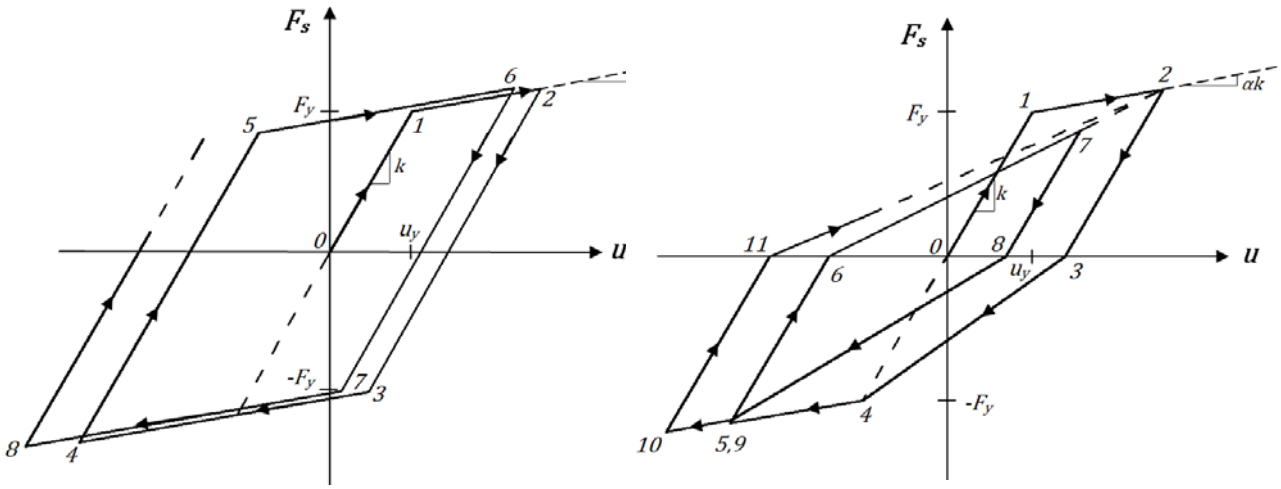

Elasto-Plastic Model
(Steel members)

Stiffness Degrading Model
(RC members)

Fig. 2.22. Elasto-plastic and stiffness degrading hysteresis models

Elasto-Plastic Model

There are two stiffness states in the elasto-plastic model (Fig. 2.22.a): k or αk. Initial loading (0-1 or 0-1') starts with the stiffness k, and when the internal resistance reaches the plastic state, the system yields and deforms along the yield plateau with post-yield stiffness αk (1-2). Unloading and reloading (2-3; 4-5; 6-7) take place along the elastic paths with the initial stiffness k. When the direction of loading changes from loading to unloading or vice versa along these paths, the stiffness does not change. On the other hand, when the internal resistance reaches the plastic state along these paths at points (3, 5 or 7), plastic deformations occur along the yield plateau with post-yield stiffness αk (3-4 or 5-6).

Stiffness Degrading Model

In the stiffness degrading model (Fig. 2.22.b), unloading and reloading stiffnesses are different. Unloading from the yield plateau takes place with the initial elastic stiffness k (2-3 or 5-6). Reloading then follows with a degraded stiffness defined from the point of complete unloading (3, 6 or 8) to the maximum deformation point in the same direction which occurred during the previous cycles (points 4, 2 or 9). Unloading from a reloading branch before reaching the yield plateau also takes place with the stiffness k (7-8).

Under an earthquake excitation, nonlinear systems can only develop a resistance bounded by their lateral yield strength F_y, but they respond at larger displacements. Consider

three SDOF systems with the same initial stiffness k and period T, subjected to the same earthquake ground motion $\ddot{u}_g$ (Fig. 2.23). Their properties, from the weakest to strongest are:

System 1: Elasto-plastic with yield strength F_{y1} and yield displacement u_{y1}

System 2: Elasto-plastic with yield strength F_{y2} and yield displacement u_{y2} $(F_{y2} > F_{y1})$

System 3: Linear elastic, i.e. $F_y = \infty$

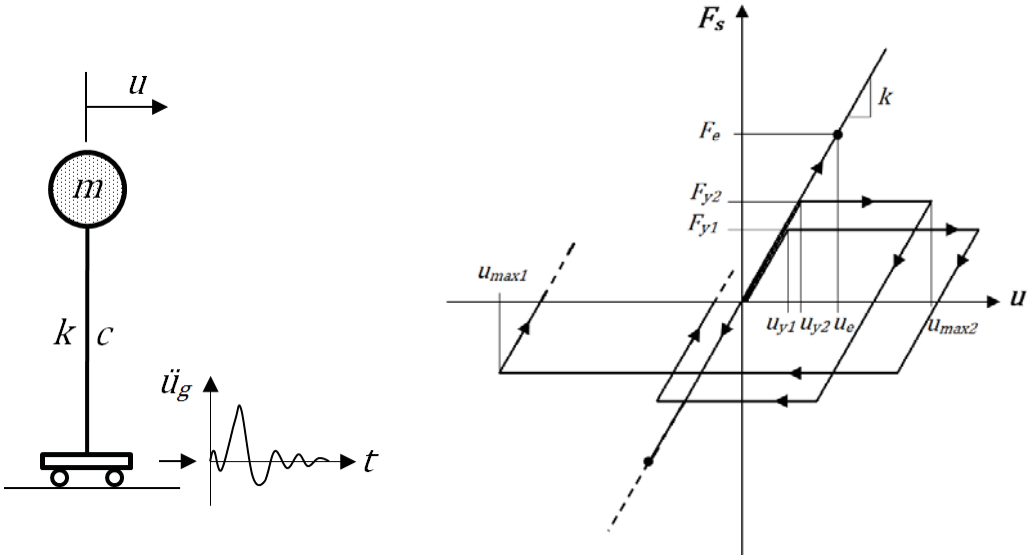

Fig. 2.23. Three SDOF systems with the same initial stiffness k, but different yield strengths F_{yi}, subjected to a strong ground excitation cycle.

We can expect that the weakest system (System 1) deforms most, to an absolute maximum displacement of u_{max1}, while system 2 deforms to a lesser maximum displacement of u_{max2}. Meanwhile the linear elastic system deforms to a maximum displacement of u_e under the same earthquake ground motion. These maximum absolute displacements u_{max1}, u_{max2} and u_e are called the *displacement demands* of the earthquake from systems 1, 2 and 3, respectively. We can also define these demands in terms of a dimensionless deformation ratio μ, called the ductility ratio.

$$\mu_i = \frac{u_{max,i}}{u_y} \tag{2.61}$$

Therefore, an earthquake ground motion demands more ductility from systems with less strength.

$$Fy_1 < Fy_2 < F_e \qquad \Rightarrow \qquad \mu_1 > \mu_2 > \mu_e \tag{2.62}$$

F_e is the elastic force demand above, and $\mu_e = 1$ theoretically for linear elastic systems.

The force terms on the left in Eq. (2.61) are the strengths (capacities) whereas the terms on the right are the ductility ratios (demands).

Example 2.6. The SDOF system given in Example 2.4 is defined as an elasto-plastic system with $F_y = 0.1mg$ and $\alpha=0$. Determine the displacement response, $u(t)$, under the same $\ddot{u}_g(t)$.

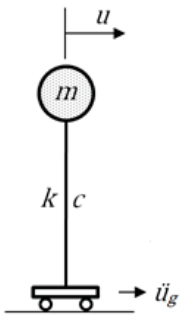

SDOF system

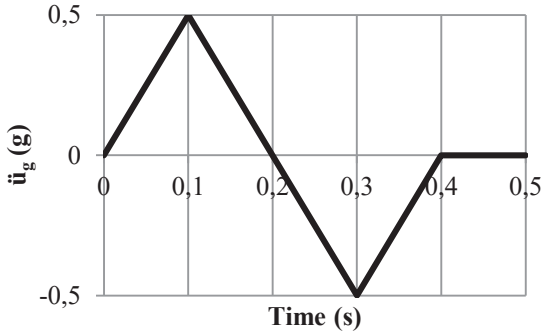

Ground Acceleration

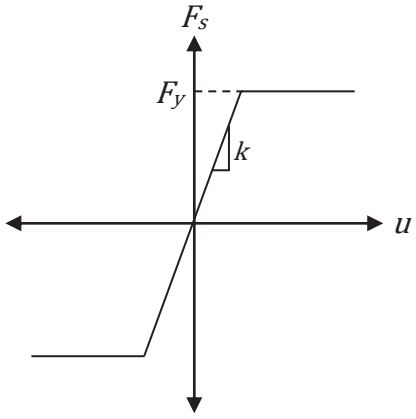

Elasto-plastic behavior

Solution: Elasto-plastic system.

m	T_n (s)	ω_n (rad/s)	ξ	Δt (s)	c	$k_{elastic}$	α	f_y	u_0	$\dot{u}_0$	$\ddot{u}_0$	$f_{s(0)}$
1	1	6,28	0,05	0,1	0,628	39,478	0	0,981	0	0	0	0

$$k_i^* = k_i + \frac{2c}{\Delta t} + \frac{4m}{\Delta t^2} \qquad \text{where } k_i \text{ is the tangent } k \text{ at } u_i.$$

$$\Delta f_{s(i)} = -m\left(\ddot{u}_{g(i+1)} - \ddot{u}_{g(i)}\right) - m\Delta\ddot{u}_i - c\Delta\dot{u}_i \qquad \ddot{u}_{i+1} = \frac{1}{m}\left(-m\ddot{u}_{g(i+1)} - c\dot{u}_{i+1} - f_{s(i+1)}\right)$$

i	t	u_i	$\dot{u}_i$	$\ddot{u}_i$	k_i	k_i^*	Δp_i^*	Δu_i	$\Delta\dot{u}_i$	$\Delta\ddot{u}_i$	
0	0	0	0	0	39,478	452,045	-4,905	-0,0109	-0,2170	-4,3403	Cont'd
1	0,1	-0,0109	-0,2170	-4,3403	39,478	452,045	-12,729	-0,0282	-0,1291	6,0978	
2	0,2	-0,0390	-0,3462	1,1985	0,000	412,566	-6,979	-0,0169	0,3540	4,6826	
3	0,3	-0,0559	0,0078	5,8811	0,000	412,566	7,180	0,0174	0,3324	-5,1139	
4	0,4	-0,0385	0,3402	0,7672							

					Calc.	Actual			
	i	t	$f_{s(i)}$	$\Delta f_{s(i)}$	$f_{s(i+1)}$	$f_{s(i+1)}$	u_{i+1}	$\dot{u}_{i+1}$	$\ddot{u}_{i+1}$
Cont'd	0	0	0	-0,428	-0,428	-0,428	-0,0109	-0,2170	-4,3403
	1	0,1	-0,428	-1,112	-1,540	-0,981	-0,0390	-0,3462	1,1985
	2	0,2	-0,981	0,000	-0,981	-0,981	-0,0559	0,0078	5,8811
	3	0,3	-0,981	0,000	-0,981	-0,981	-0,0385	0,3402	0,7672
	4	0,4							

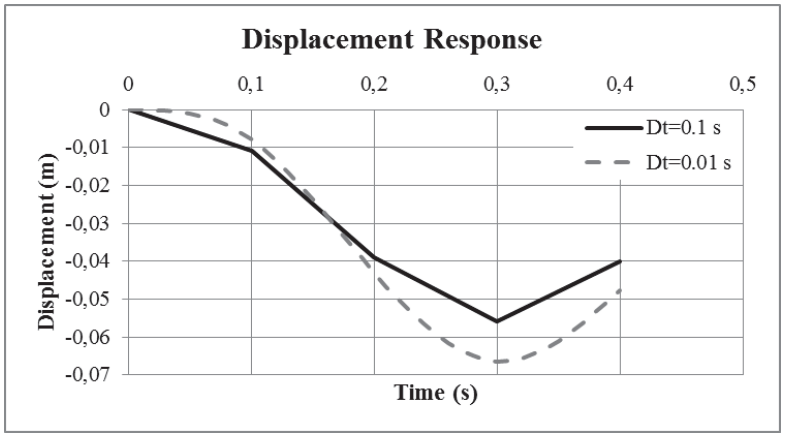

2.6.3 Ductility and Strength Spectra for Nonlinear SDOF Systems

We can solve the nonlinear equation of motion

$$m\ddot{u} + c\dot{u} + f_s(u) = -m\ddot{u}_g(t) \tag{2.63}$$

for different elasto-plastic systems with the same F_y and ξ, but different k_i *(or* T_i *)* under the same earthquake ground motion $\ddot{u}_g$. Accordingly, we can obtain the maximum displacement $u_{max,i}$ corresponding to each system with k_i , or T_i. This is schematized in Fig. 2.24 under a strong ground excitation cycle.

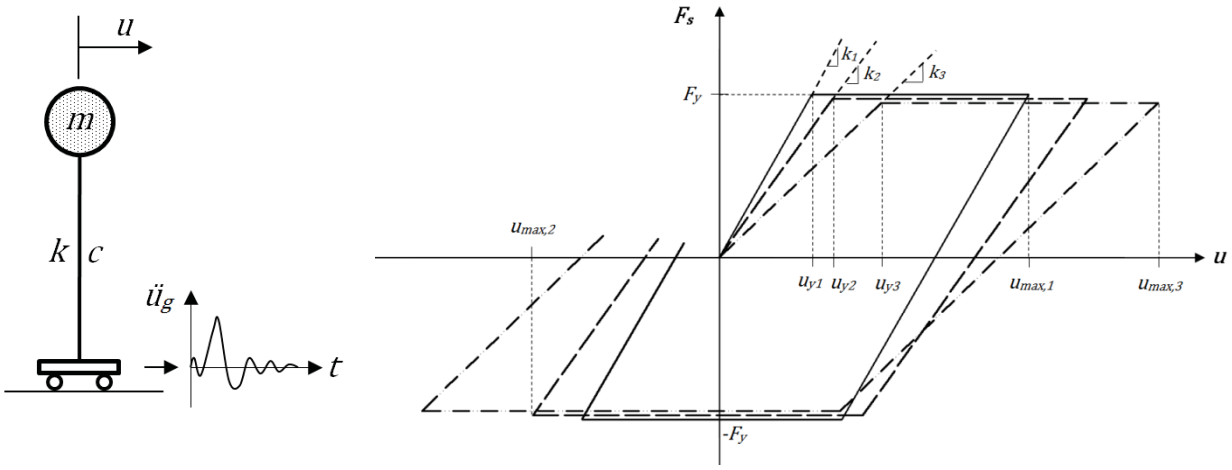

Fig. 2.24. Three SDOF systems with the same strength F_y, but different initial stiffnesses k_i, subjected to a strong ground excitation cycle.

Then, $\mu_i = \frac{u_{\max i}}{u_{y\,i}}$ versus T_i can be plotted as a spectrum, called the ductility spectrum. If this process is repeated for different F_y values, we obtain *ductility spectra* for constant strength values F_y. The F_y values are usually expressed as a ratio of *mg* in these charts. Ductility spectra obtained for the Düzce 1999 ground motion is shown in Fig. 2.25.

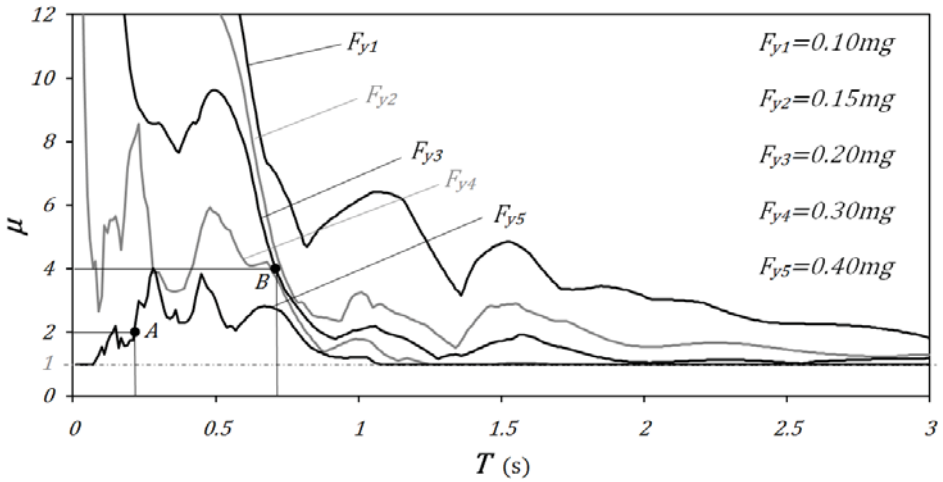

Fig. 2.25. Ductility spectra of the 1999 Düzce NS ground motion for different constant strength ratios.

Next, we can convert the μ - T (ductility) spectra to a F_y – T (strength) spectra by graphical interpolation. If we assume a constant ductility value on Fig. 2.25, it intersects each F_y curve at a different T value. Hence, a set of F_y-T values are obtained for a constant ductility ratio of μ. We can plot the set of F_y-T values for constant ductility as the strength spectrum. When this process is repeated for different constant ductility values, a family of constant ductility curves is obtained which is called the *strength spectra*. The strength spectra obtained for the Düzce 1999 ground motion is shown in Fig. 2.26. This graphics is also called the *inelastic acceleration spectra* (S_{ai} – T) for constant ductility μ.

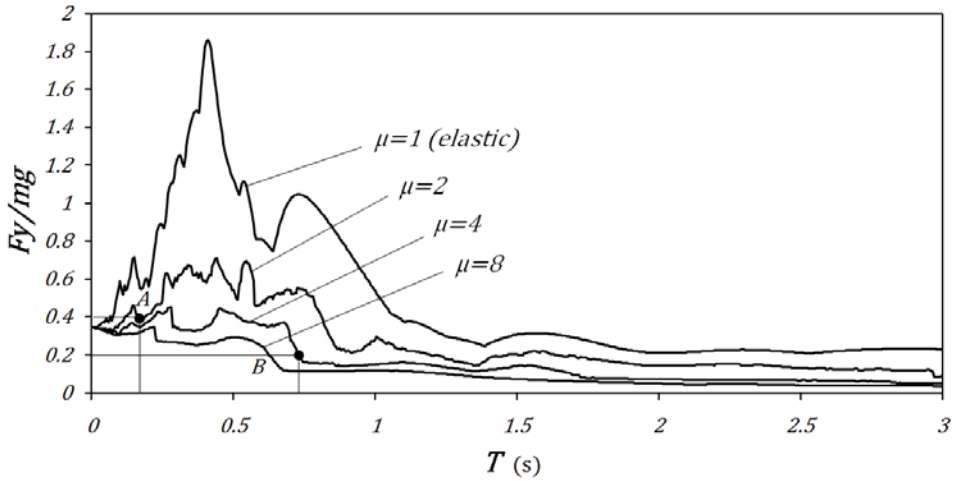

Fig. 2.26. Strength spectra or inelastic acceleration spectra of the 1999 Düzce NS ground motion for different constant ductility ratios.

The correspondence between the ductility spectra in Fig. 2.25 and the strength spectra in Fig. 2.26 can be explained with a simple example. Point *A* in Fig. 2.25 is on the F_y *=0.40 mg* curve at T= 0.21 s with μ=2. Similarly, point *B* is on the F_y *=0.20 mg* curve at T= 0.71 s with μ=4. These two points are also marked on Fig. 2.26, at the same period values on the corresponding constant ductility curves for μ=2 and 4. Their F_y values are exactly the same.

If we know the period T and strength F_y of our SDOF system, then we can directly calculate the ductility demand of the earthquake from the inelastic acceleration spectra. On the other hand, if we have a given (estimated) ductility capacity μ for our system, then we can determine the required (minimum) strength for not exceeding this ductility capacity under the considered ground motion. This is very suitable for the force-based seismic design.

2.6.4 Ductility Reduction Factor (R_μ)

R_μ is defined as the ratio of elastic force demand F_e to the yield capacity F_y of the nonlinear SDOF system with the same initial stiffness k, under the same earthquake ground excitation $\ddot{u}_g$ (Eq. 2.64), which is depicted in Fig. 2.27.

$$R_\mu = \frac{F_e}{F_y} \tag{2.64}$$

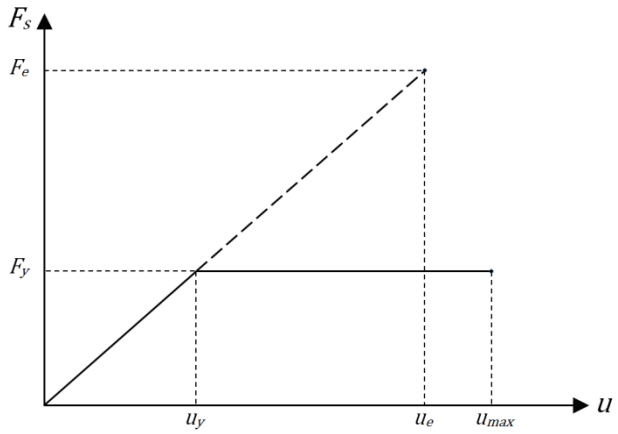

Fig. 2.27. Force-displacement responses of a linear elastic and a nonlinear SDOF system under an earthquake ground excitation $\ddot{u}_g$.

There is a corresponding ductility demand $\mu = \frac{u_{max}}{u_y}$ from the nonlinear system with the initial stiffness $k=F_y/u_y$ and the initial period $T = \frac{1}{2\pi}\sqrt{\frac{m}{k}}$. If this process is repeated for several nonlinear systems with different F_y and T values as in Fig. 2.23, a set of $R_\mu - \mu - T$ curves can be obtained, which can be plotted as a spectra. The $R_\mu - \mu - T$ spectra obtained for the Düzce 1999 and El Centro 1940 ground motions are shown in Fig. 2.28.

Usually it is observed that R_μ oscillates around μ when $T > T_c$ where T_c is called the *corner period* of the ground motion. Then $R_\mu \to \mu$ when $T > T_c$. This assumption is valid for the mean $R_\mu - \mu - T$ spectrum of many ground motions, although it is a crude approximation for a single ground motion.

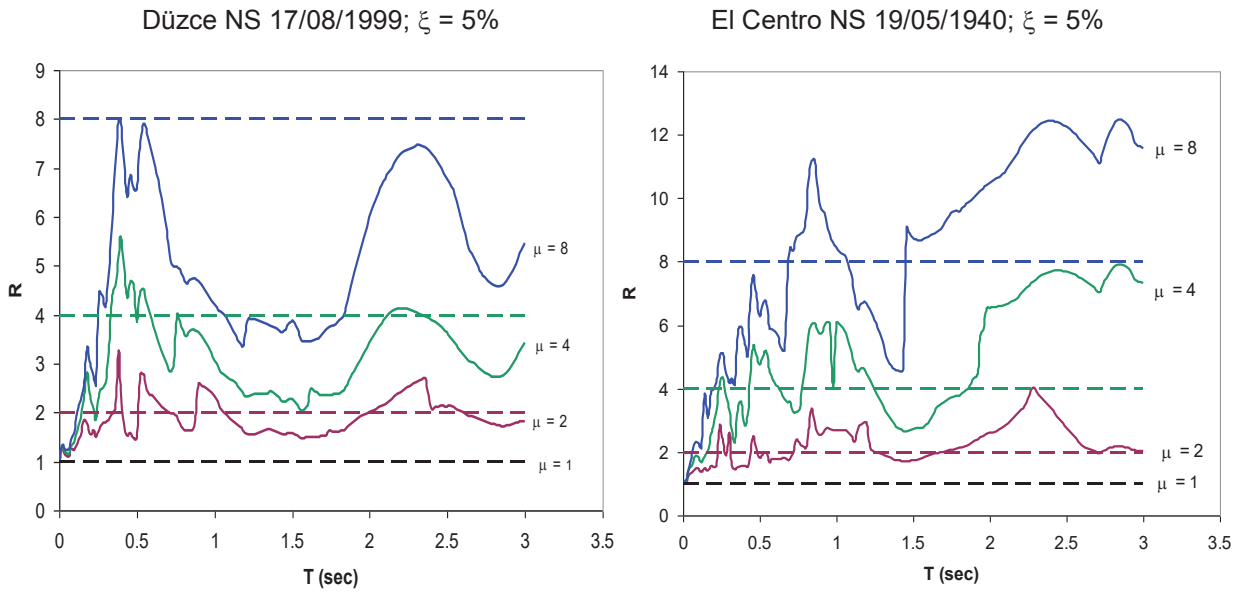

Fig. 2.28. $R_\mu - \mu - T$ spectra of the 1999 Düzce NS and 1940 El Centro NS ground motion components for different constant ductility ratios.

The mean $R_\mu - \mu - T$ spectrum can be idealized in a simple form shown in Fig. 2.29.

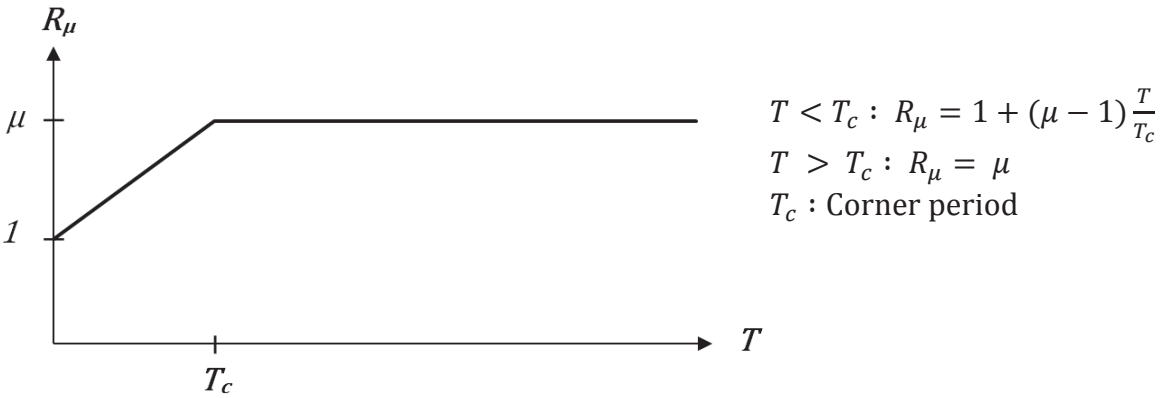

Fig. 2.29. Idealized form of the $R_\mu - \mu - T$ spectrum.

By using an exact $R_\mu - \mu - T$ spectrum, or the idealized one, we can obtain the inelastic acceleration spectrum S_{ai} and inelastic displacement spectrum S_{di} from the corresponding linear elastic acceleration and displacement spectrum, S_{ae} and S_{de}, respectively. If we exploit the identities

$$R_\mu = \frac{F_e}{F_y} = \frac{F_e/m}{F_y/m} = \frac{S_{ae}}{S_{ai}} \quad \text{and} \quad R_\mu = \frac{F_e}{F_y} = \frac{ku_e}{ku_y} = \frac{S_{de}}{S_{di}/\mu}$$

we obtain

$$S_{ai} = \frac{S_{ae}}{R_\mu} \quad \text{and} \quad S_{di} = \frac{\mu}{R_\mu}.S_{de} \qquad (2.65.\ a, b)$$

Eq. (2.65.a) can be employed for obtaining the inelastic acceleration response spectra S_{ai} directly from the linear elastic acceleration spectrum S_{ae} by selecting an R_μ ratio. This is very practical for seismic design since R_μ factors for different types of structural systems are defined in seismic design codes. Similarly, inelastic displacement response spectra S_{di} can be obtained from the linear elastic displacement response spectrum S_{de} by using Eq. (2.65.b). Inelastic acceleration (yield acceleration) spectra and inelastic displacement spectra calculated for the Düzce 1999 ground motion by employing Eqs. (2.65) are shown in Figs. 2.30.a and 2.30.b respectively for several R_μ factors.

It is noteworthy to compare the strength spectra in Fig. 2.26 with the yield acceleration spectra in Fig. 2.30.a. In an elasto-plastic system, strength and yield acceleration are related through $F_y=ma_y$. However the inelastic spectral curves are slightly different at short periods. If R_μ was not constant for each curve in Fig. 2.30.a but it was a function of period as in Fig. 2.28.a, then the two spectra would be the same.

Fig. 2.30.b implies that the response displacements of linear elastic and inelastic SDOF systems are very close. This property is discussed further in the following section.

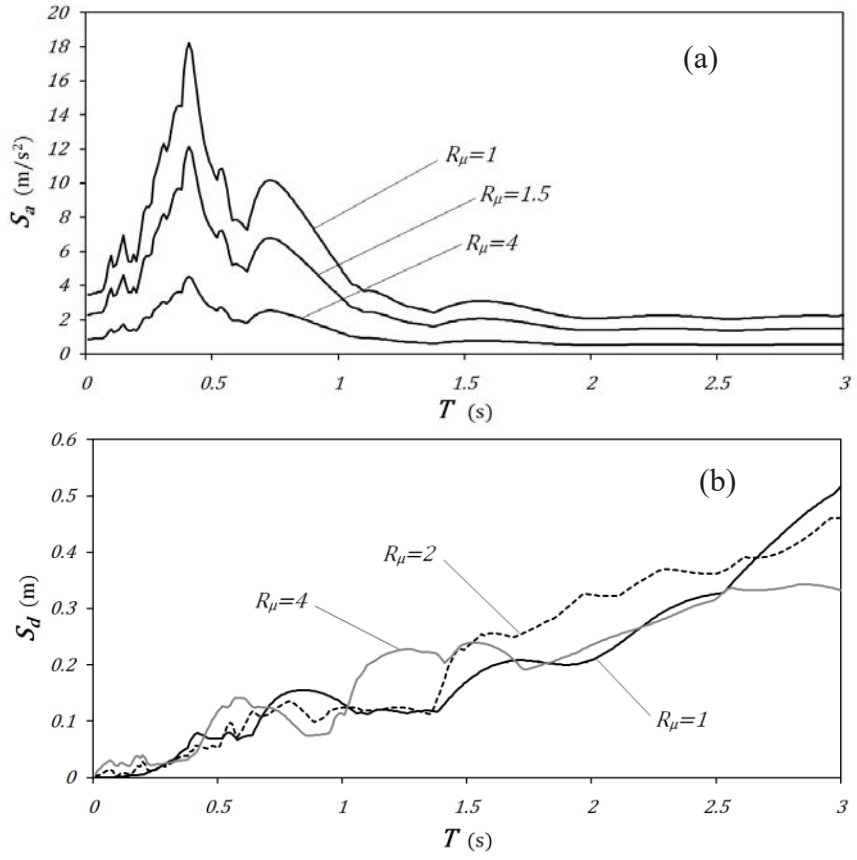

Fig. 2.30. Inelastic acceleration (yield acceleration) and displacement response spectra of the 1999 Düzce NS ground motion component for different R_μ factors.

2.6.5 Equal Displacement Rule

For medium and long period SDOF systems ($T > 0.5$ second), $R_\mu = \mu$ implies the "*equal displacement rule*", which is derived in Eq. (2.66) below with the aid of Fig. 2.31, Eqs. (2.61) and (2.64).

$$k = \frac{F_e}{u_e} = \frac{F_y}{u_y} \Rightarrow \frac{F_e}{F_y} = \frac{u_e}{u_y} \equiv \frac{u_{max}}{u_y} \Rightarrow R_\mu = \mu \tag{2.66}$$

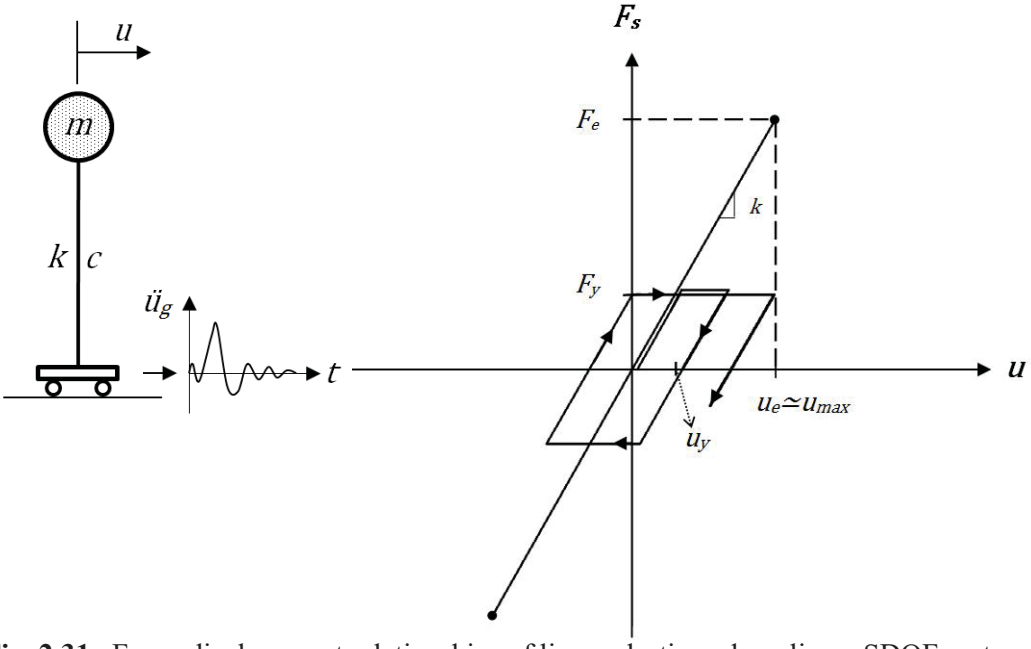

Fig. 2.31. Force-displacement relationships of linear elastic and nonlinear SDOF systems under a ground excitation. $u_e \approx u_{max}$ implies the equal displacement rule.

Equal displacement rule can be simply tested by plotting the variation of inelastic displacement ratio u_{max} / u_e with T which is shown in Fig. 2.32 for the ground motions employed in Fig. 2.18. The rule is verified for $T > 0.1$ second since the mean u_{max} / u_e ratio approaches unity after this period.

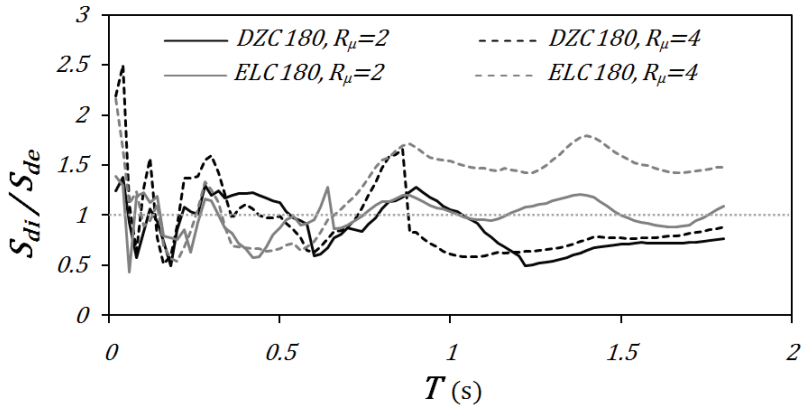

Fig. 2.32. Variation of inelastic-to-elastic maximum displacement ratio with period.

3.

Response of Building Structures to Earthquake Ground Motions

3.1 INTRODUCTION

Building structures are multi degree of freedom (MDOF) systems where more than one displacement coordinate is necessary for defining the position of the system during motion.

The minimum number of displacement coordinates required to define the deflected shape of the system properly at any time "t" during motion is the number of "*degrees of freedom*", DOF. They are the independent coordinates (displacement $u(t)$, rotation $\theta(t)$, etc.) that change with time.

3.2 EQUATIONS OF MOTION

We will develop the equation of motion of a MDOF system by employing a shear frame for brevity. A shear frame is a single-bay, N-story frame consisting of flexible columns and fully rigid girders where the story masses are assigned to the girders. An N-story shear frame under base excitation $\ddot{u}_g(t)$ is shown in Fig. 3.1. Since the girders are rigid, there are no joint rotations at the joints and transverse displacements at both ends of a girder are identical. Accordingly only one degree of freedom u_i is sufficient for each story i, which is along the girder where the mass m_i is assigned. Each story i has a total shear stiffness k_i that is composed of the column shear stiffnesses $12EI/h^3$ in that story.

The equation of motion under base excitation has the same form with Eq. (2.5), where the scalar displacement variables $u, \dot{u}$ and $\ddot{u}$ for a SDOF system are replaced with the vectorial displacement variables $\underline{u}$, $\underline{\dot{u}}$ and $\underline{\ddot{u}}$ for a MDOF system. Similarly, the scalar mass, stiffness and damping property terms are replaced with the associated matrix quantities:

$$\underline{m}\,\underline{\ddot{u}}^{total} + \underline{c}\,\underline{\dot{u}} + \underline{k}\,\underline{u} = \underline{0} \tag{3.1}$$

where

$$\underline{\ddot{u}}^{total} = \underline{\ddot{u}} + \ddot{u}_g.\underline{l} \quad \text{and} \quad \underline{l} = \begin{Bmatrix} 1 \\ 1 \\ \vdots \\ 1 \end{Bmatrix} \tag{3.2}$$

The vector $\underline{l}$ is transmitting the ground displacement u_g to the story DOF's above as rigid body displacements. It is called the influence vector. $\underline{l}$ = $\underline{1}$ for shear frames since a unit displacement at the ground is transmitted equally to all DOF's defined at the stories above.

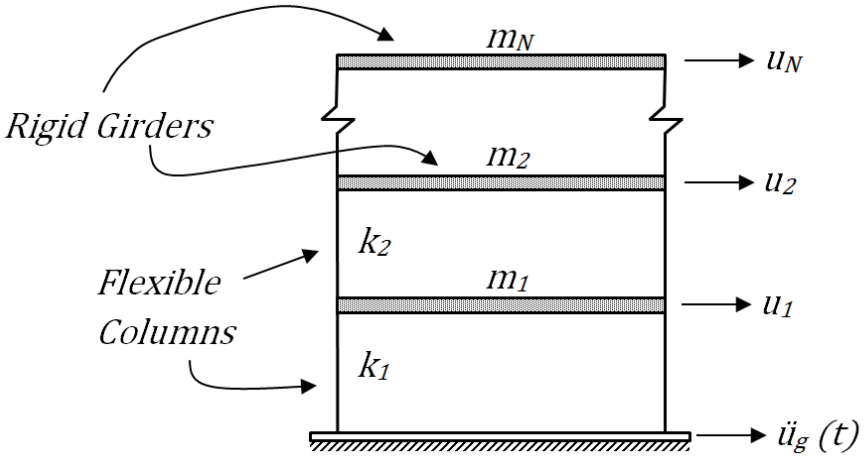

Fig. 3.1. An N-story shear frame subjected to the ground excitation $\ddot{u}_g\,(t)$

When $\underline{\ddot{u}}^{total}$ and $\underline{l}$ are substituted from Eq. (3.2) into Eq. (3.1), we obtain

$$\underline{m}\,\underline{\ddot{u}} + \underline{c}\,\underline{\dot{u}} + \underline{k}\,\underline{u} = -\underline{m}\,\underline{l}\,\ddot{u}_g \tag{3.3}$$

where

$$\underline{m} = \begin{bmatrix} m_1 & 0 & \cdots & 0 \\ 0 & m_2 & & 0 \\ \vdots & & \ddots & \vdots \\ 0 & 0 & \cdots & m_N \end{bmatrix} \tag{3.4}$$

is the mass matrix, and

$$\underline{k} = \begin{bmatrix} (k_1 + k_2) & -k_2 & & & \\ -k_2 & (k_2 + k_3) & -k_3 & & \\ & & \ddots & & \\ & & & -k_{N-1} & (k_{N-1} + k_N) & -k_N \\ & & & & -k_N & k_N \end{bmatrix} \tag{3.5}$$

is the stiffness matrix. Each stiffness coefficient k_i in Eq. (3.5) represents the total lateral stiffness of the i'th story that is composed of the column shear stiffnesses as indicated above.

$$k_i = \sum 12 \left(\frac{EI}{h^3}\right)_i \tag{3.6}$$

The displacement vector is composed of the N lateral story displacements (degrees of freedom).

$$\underline{u}(t) = \begin{Bmatrix} u_1(t) \\ u_2(t) \\ \vdots \\ u_N(t) \end{Bmatrix} \tag{3.7}$$

It should be noted that the mass matrix in Eq. (3.4) is a lumped matrix which is indicating no coupling between the story masses. Moreover, the stiffness matrix in Eq. (3.5) is tri-diagonal, hence the lateral stiffness of a story is coupled with the lateral stiffnesses of the story below and above only (close-coupling). These are inherent properties of the shear frame in Fig. 3.1.

There is no analytical method for obtaining the coefficients of the damping matrix $\underline{c}$ in Eq. (3.3) from the damping properties of structural members. There is a practical approach for obtaining the damping matrix of a MDOF system, called Rayleigh damping (Chopra 2001, Chapter 11). The construction of damping matrix is not required however in the following approach.

3.3 UNDAMPED FREE VIBRATION: EIGENVALUE ANALYSIS

When the force term on the right-hand-side of Eq. (3.3) is zero and the damping is ignored, we obtain the undamped free vibration equation:

$$\underline{m}\,\ddot{\underline{u}} + \underline{k}\,\underline{u} = \underline{0} \tag{3.8}$$

Free vibration can be induced by the initial conditions at t=0.

$$\underline{u}(0) = \underline{u}_0\,, \quad \dot{\underline{u}}(0) = \underline{v}_0 \tag{3.9}$$

If we can impose a "special" initial shape $\underline{u}_0$, then we observe harmonic free vibration (simple harmonic motion) with a fixed displacement profile along the height. A fixed profile indicates fixed proportionality of the story displacements with respect to each other. Vibration with a fixed displacement profile is identical to a single degree of freedom response which was previously discussed in Section **2.1** and shown in Fig. 3.2.b and c. These special displacement profiles are the *"natural mode shapes*", and their corresponding harmonic

vibration frequencies are the "*natural frequencies of vibration*". There are N such mode shapes for an N-DOF system. Typical displacement profiles representing such mode shapes are illustrated in Figs. 3.2.b and 3.2.c for a three story shear frame. When free vibration is induced with a non-special, or general initial displacement shape, then the profile of this initial shape cannot be retained during free vibrations, and a modality does not develop as shown in Fig. 3.2.d.

We have to carry out eigenvalue analysis for determining the natural mode shapes and natural vibration frequencies.

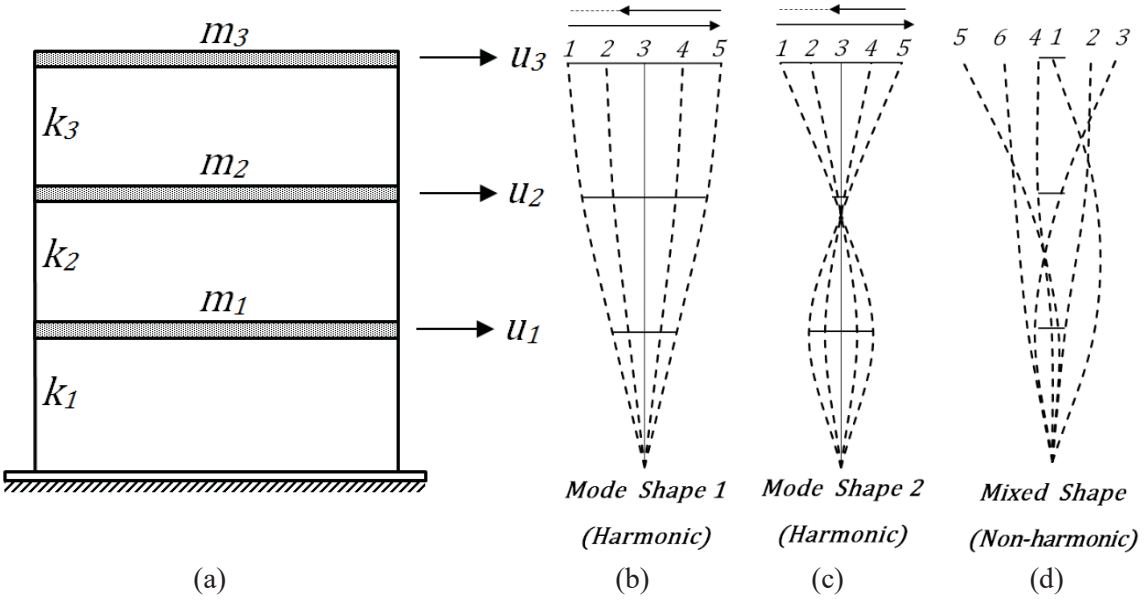

Fig. 3.2. A 3-story shear frame in free vibration. (a) Shear frame properties, (b) and (c) harmonic free vibrations with special initial shapes, (d) non-harmonic free vibration where the initial shape degenerates. Numbers on top indicate time sequence of deflections.

3.3.1 Vibration Modes and Frequencies

At a given mode, the displacement vector varies harmonically with time whereas its shape profile remains "fixed". Then, we can express the modal displacement vector as the product of a harmonic function of time and a shape function.

$$\underline{u_n}(t) = q_n(t) \cdot \underline{\phi_n} \tag{3.10}$$

Here, $\underline{\phi_n}$ describes the displacement profile along the height, or the mode shape whereas $q_n(t)$ is the time dependent amplitude of this profile. Their product in Eq. (3.10) gives the

modal displacement shape for a mode n at any time t during free vibration. This assumption is analogous to the method of "separation of variables" in solving partial differential equations.

Since free vibration motion with a mode shape is harmonic, we can assume a harmonic function for $q_n(t)$.

$$q_n(t) = A_n \cos \omega_n t + B_n \sin \omega_n t \tag{3.11}$$

When $q_n(t)$ is substituted from Eq. (3.11) into Eq. (3.10) and the displacement vector in Eq. (3.10) is differentiated twice with respect to time, an expression for acceleration vector is obtained.

$$\underline{\ddot{u}}_n(t) = \ddot{q}_n(t) \cdot \underline{\phi}_n = -\omega_n^2 \, q_n(t) \cdot \underline{\phi}_n \equiv -\omega_n^2 \, u_n(t) \tag{3.12}$$

In Eq. (3.12), $\underline{\phi}_n$ and ω_n are the modal vibration frequency (eigenvalue) and mode shape (eigenvector) of the n'th mode, which have to be determined through an inverse solution approach.

Substituting $\underline{u}$ and $\underline{\ddot{u}}$ from Eqs. (3.10) and (3.12) respectively into the equation of free vibration motion (3.8), we obtain

$$\left(-\omega_n^2 \, \underline{m} \, \underline{\phi}_n + \underline{k} \, \underline{\phi}_n\right) q_n(t) = \underline{0} \tag{3.13}$$

Here, $q_n = 0$ is not an acceptable solution for Eq. (3.13), because it implies no vibration (trivial solution). Therefore,

$$-\omega_n^2 \, \underline{m} \, \underline{\phi}_n + \underline{k}\underline{\phi}_n = \underline{0} \tag{3.14.a}$$

or

$$(\underline{k} - \omega_n^2 \, \underline{m}) \cdot \underline{\phi}_n = \underline{0} \tag{3.14.b}$$

This is a set of N-homogeneous algebraic equations. $\underline{\phi}_n = \underline{0}$ is also a trivial solution (no deformation) for Eq. (3.14). A non-trivial solution is possible only if the determinant of $(\underline{k} - \omega_n^2 \, \underline{m})$ is zero (*Cramer's Rule*):

$$\left|\underline{k} - \omega_n^2 \, \underline{m}\right| = 0 \tag{3.15}$$

Eq. (3.15) is equivalent to an N^{th} order algebraic equation with N roots. The ω_n^2 values are the roots, or the eigenvalues (n=1, 2, …. N). If ω_n^2 is known for a mode n, then we can determine the corresponding shape vector $\underline{\phi}_n$ from Eq. (3.14).

Summary

For an N-DOF structural system, there are N pairs of eigenvalues and eigenvectors $(\omega_n^2, \underline{\phi}_n)$, n=1, 2, ….. N. Their values are related to the mass and stiffness properties of the system. The system can vibrate in a simple harmonic motion independently at each mode, with the profile $\underline{\phi}_n$ at the associated angular frequency ω_n.

Example 3.1. A 2DOF system is given in Figures (a) and (b), which are dynamically identical. Determine its eigenvalues and eigenvectors.

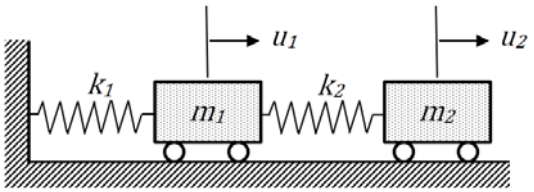

(a)

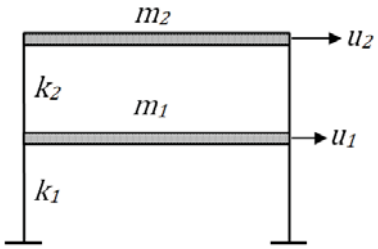

(b)

The equation of motion for free vibration, from Eq. (3.8), can be written as

$$\begin{bmatrix} m_1 & 0 \\ 0 & m_2 \end{bmatrix} \begin{Bmatrix} \ddot{u}_1 \\ \ddot{u}_2 \end{Bmatrix} + \begin{bmatrix} k_1 + k_2 & -k_2 \\ -k_2 & k_2 \end{bmatrix} \begin{Bmatrix} u_1 \\ u_2 \end{Bmatrix} = \begin{Bmatrix} 0 \\ 0 \end{Bmatrix} \tag{1}$$

Then Eq. (3.15) is applied to the given problem.

$$\det\left(\underline{k} - \omega_n^2 \underline{m}\right) = \begin{vmatrix} (k_1 + k_2 - \omega_n^2 m_1) & -k_2 \\ -k_2 & k_2 - \omega_n^2 m_2 \end{vmatrix} = 0 \tag{2}$$

A closed form solution cannot be determined from Eq. (2). This is possible however if we make a simplification in the parameters. Let $k_1 = k_2 = k$, and $m_1 = m_2 = m$. Then Eq. (3) can be obtained from Eq. (2), which is called the *characteristic equation*.

$$\omega_n^4 - 3\frac{k}{m}\omega_n^2 + \left(\frac{k}{m}\right)^2 = 0 \tag{3}$$

Eq. (3) is a quadratic algebraic equation in ω_n^2 where n=1, 2. The roots of the quadratic equation are ω_1^2 and ω_2^2, which are the eigenvalues (note that the roots are <u>not</u> ω_1 *and* ω_2). Solution of Eq. (3) yields the following roots:

$$\omega_1^2 = \frac{3-\sqrt{5}}{2}\frac{k}{m} \quad \rightarrow \quad \omega_1 = 0.618\sqrt{\frac{k}{m}} \tag{4}$$

$$\omega_2^2 = \frac{3+\sqrt{5}}{2}\frac{k}{m} \quad \rightarrow \quad \omega_2 = 1.618\sqrt{\frac{k}{m}} \tag{5}$$

The eigenvectors will be determined from Eq. (3.14). For the given problem,

$$\begin{bmatrix}(2k-\omega_n^2 m) & -k \\ -k & k-\omega_n^2 m\end{bmatrix}\begin{Bmatrix}\phi_{n1}\\ \phi_{n2}\end{Bmatrix}=\begin{Bmatrix}0\\0\end{Bmatrix} \quad ; \quad n=1,2 \tag{6}$$

From row 1; $$(2k-\omega_n^2 m)\phi_{n1} - k\,\phi_{n2} = 0 \tag{7}$$

From row 2 : $$-k\,\phi_{n1} + (k-\omega_n^2 m)\phi_{n2} = 0 \tag{8}$$

We cannot find a unique solution for ϕ_{n1} and ϕ_{n2} from Eqs. (7) and (8) because they are a set of homogeneous equations. We can rather express ϕ_{n2} in terms of ϕ_{n1} for both n=1 and n=2.

$$\phi_{n2} = \frac{2k-\omega_n^2 m}{k}\,\phi_{n1} \tag{9}$$

Let $\phi_{n1} = 1$ in Eq. (9) for n=1 and n=2. Then we first substitute ω_1^2 into Eq. (9) and determine $\phi_{12} = 1.618$. Next, we substitute ω_2^2 into Eq. (9) and determine $\phi_{22} = -0.618$. Accordingly, the modal vectors, or the eigenvectors for the two modes are determined.

$$\underline{\phi}_1 = \begin{Bmatrix}1.0\\1.618\end{Bmatrix}; \quad \underline{\phi}_2 = \begin{Bmatrix}1.0\\-0.618\end{Bmatrix} \tag{10}$$

The mode shapes for the 2DOF system in Fig. (b) are plotted below.

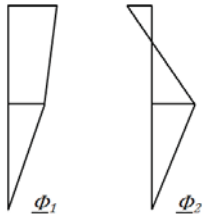

Example 3.2. Identify the degrees of freedom of the system given in Figure (a). Then determine its eigenvalues and eigenvectors.

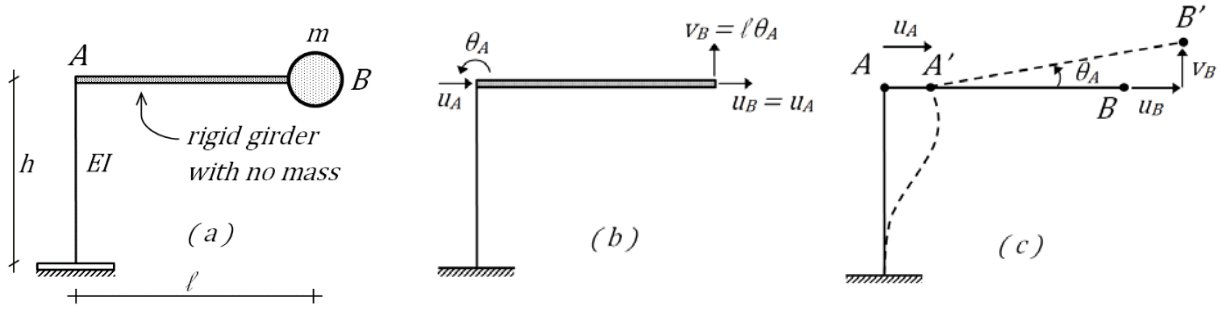

Solution

The frame has 2 DOF's, which are defined at the top end A of the cantilever column and shown in Fig. (b). Although this is correct and consistent for static analysis, we have to transfer these DOF's to point B for dynamic analysis since the point mass is assigned to the B end of the rigid girder. The original (u_A, θ_A) and the transferred (new) degrees of freedom (u_B, v_B) are shown in Fig. (b). Note that these two sets of DOF's are dependent since u_B=u_A (rigid

body translation of AB) and $v_B = l\,\theta_A$ (rigid body rotation of AB). The kinematic relation between (u_B, v_B) and (u_A, θ_A) is sketched in Fig. (c).

The stiffness equations for the first and second set of DOF's can be written as (determine as an exercise),

$$\begin{bmatrix} F_{hA} \\ M_A \end{bmatrix} = \frac{EI}{h}\begin{bmatrix} \frac{12}{h^2} & \frac{6}{h} \\ \frac{6}{h} & 4 \end{bmatrix}\begin{bmatrix} u_A \\ \theta_A \end{bmatrix} \quad and \quad \begin{bmatrix} F_{hB} \\ F_{vB} \end{bmatrix} = \frac{EI}{h}\begin{bmatrix} \frac{12}{h^2} & \frac{6}{hl} \\ \frac{6}{hl} & \frac{4}{l^2} \end{bmatrix}\begin{bmatrix} u_B \\ v_B \end{bmatrix} \qquad (1.a, b)$$

Then the mass and stiffness matrices for the second set of DOF's are,

$$\underline{m} = \begin{bmatrix} m & 0 \\ 0 & m \end{bmatrix} \qquad \underline{k} = \frac{EI}{h}\begin{bmatrix} \frac{12}{h^2} & \frac{6}{hl} \\ \frac{6}{hl} & \frac{4}{l^2} \end{bmatrix} \qquad (2.a, b)$$

Let's assume l=h for simplicity. Then $det\left(\underline{k} - \omega_n^2\,\underline{m}\right) = 0$ gives,

$$m^2\lambda_n^2 - \frac{16EI}{h^3}m\lambda_n + \frac{12(EI)^2}{h^6} \qquad (3)$$

In Eq. (3), $\lambda_n = \omega_n^2$. The two roots of the quadratic Eq. (3) can be determined as

$$\lambda_1 \equiv \omega_1^2 = 0.789\left(\frac{EI}{mh^3}\right) \quad and \quad \lambda_2 \equiv \omega_2^2 = 15.211\left(\frac{EI}{mh^3}\right)$$

Substituting ω_1^2 and ω_2^2 into Eq. (3.14) and solving the homogeneous set of linear equations, we obtain the two eigenvectors.

$$n=1: \quad \phi_{11} = 1; \quad \phi_{12} = -1.869$$

$$n=2: \quad \phi_{21} = 1; \quad \phi_{22} = 0.535$$

The mode shapes are sketched below.

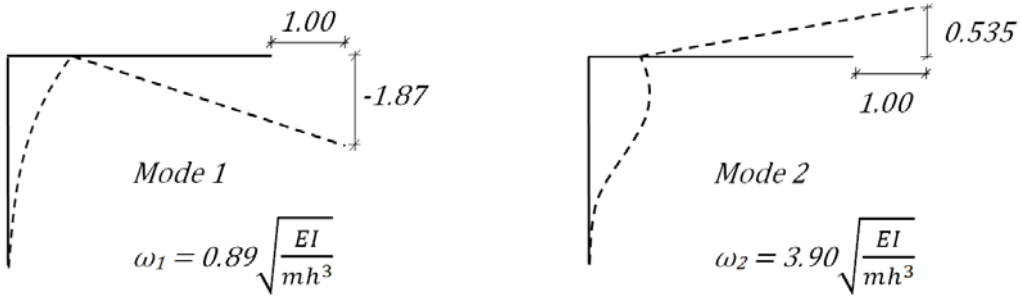

3.3.2 Normalization of Modal Vectors

Let $\underline{\phi}_n^T \underline{m} \underline{\phi}_n = M_n$ where M_n is called the n^{th} *modal mass*. If we divide $\underline{\phi}_n$ by $\sqrt{M_n}$; then

$$\frac{1}{\sqrt{M_n}} \underline{\phi}_n^T \underline{m} \frac{1}{\sqrt{M_n}} \underline{\phi}_n = 1 \tag{3.16}$$

The modal vector $\left(\frac{1}{\sqrt{M_n}} \underline{\phi}_n\right)$ is now normalized with respect to the modal mass M_n. This is practical in numerical applications because it reduces the amount of arithmetical computations. Most of the computational software directly calculates mass normalized modal vectors in earthquake engineering practice.

Example 3.3. Consider Example 3.1. Calculate the mass normalized modal vectors.

$$M_1 = \{1.0 \quad 1.618\} \begin{bmatrix} m & 0 \\ 0 & m \end{bmatrix} \begin{Bmatrix} 1.0 \\ 1.618 \end{Bmatrix} = 3.618\, m$$

$$M_2 = \{1.0 \quad -0.618\} \begin{bmatrix} m & 0 \\ 0 & m \end{bmatrix} \begin{Bmatrix} 1.0 \\ -0.618 \end{Bmatrix} = 1.382\, m$$

The mass parameter m can be neglected in both M_n terms since m is arbitrary. Then,

$$\underline{\phi}_1 = \frac{1}{\sqrt{3.618}} \begin{Bmatrix} 1.0 \\ 1.618 \end{Bmatrix} = \begin{Bmatrix} 0.526 \\ 0.851 \end{Bmatrix} \quad \text{and} \quad \underline{\phi}_2 = \frac{1}{\sqrt{1.382}} \begin{Bmatrix} 1.0 \\ -0.618 \end{Bmatrix} = \begin{Bmatrix} 0.851 \\ -0.576 \end{Bmatrix}$$

are the normalized modal vectors. It can be verified that the normalized modal vectors satisfy

$$\underline{\phi}_1^T \underline{m} \underline{\phi}_1 = 1 \text{ and } \underline{\phi}_2^T \underline{m} \underline{\phi}_2 = 1$$

Hence, $M_n = 1$ for mass-normalized modal vectors.

3.3.3 Orthogonality of Vibration Modes

Let's consider two modes *n* and *m*, with $\left(\omega_n^2, \underline{\phi}_n\right)$ and $\left(\omega_m^2, \underline{\phi}_m\right)$. From Eq. (3.14.a),

$$\underline{k} \underline{\phi}_n = \omega_n^2 \underline{m} \underline{\phi}_n \qquad \text{and} \qquad \underline{k} \underline{\phi}_m = \omega_m^2 \underline{m} \underline{\phi}_m \tag{3.17. a, b}$$

Pre-multiplying Eq. (3.15.a) with $\underline{\phi}_m^T$ and Eq. (3.17.b) with $\underline{\phi}_n^T$ respectively,

$$\underline{\phi}_m^T \underline{k} \underline{\phi}_n = \omega_n^2 \underline{\phi}_m^T \underline{m} \underline{\phi}_n \qquad \text{and} \qquad \underline{\phi}_n^T \underline{k} \underline{\phi}_m = \omega_m^2 \underline{\phi}_n^T \underline{m} \underline{\phi}_m \tag{3.18. a, b}$$

Now, transposing both sides of Eq. (3.18.b) and considering that $\underline{k}^T = \underline{k}$ and $\underline{m}^T = \underline{m}$ due to the symmetry of both matrices,

$$\underline{\phi}_m^T \underline{k}\, \underline{\phi}_n = \omega_m^2\, \underline{\phi}_m^T \underline{m}\, \underline{\phi}_n \tag{3.19}$$

Finally, subtracting Eq. (3.19) from Eq. (3.18.a),

$$0 = (\omega_n^2 - \omega_m^2)\, \underline{\phi}_m^T \underline{m}\, \underline{\phi}_n \tag{3.20}$$

Since $\omega_n^2 \neq \omega_m^2$ in general,

$$\underline{\phi}_m^T \underline{m}\, \underline{\phi}_n = 0 \tag{3.21}$$

This is the condition of orthogonality of modal vectors with respect to the mass matrix. A similar orthogonality condition with respect to the stiffness matrix follows from Eq. (3.19).

$$\underline{\phi}_m^T \underline{k}\, \underline{\phi}_n = 0 \tag{3.22}$$

Therefore modal vectors are orthogonal with respect to $\underline{m}$ and $\underline{k}$.

Example 3.4. Consider Example 3.1. Verify orthogonality of modal vectors with respect to the mass matrix.

$$\underline{\phi}_1^T \underline{m}\, \underline{\phi}_2 = \{1.0 \quad 1.618\} \begin{bmatrix} m & 0 \\ 0 & m \end{bmatrix} \begin{Bmatrix} 1.0 \\ -0.618 \end{Bmatrix} = 0 \qquad check!$$

A similar orthogonality condition can also be verified for Example 3.2.

3.3.4 Modal Expansion of Displacements

Any displacement vector $\underline{u}(t)$ can be expressed as a linear combination of the orthogonal modal vectors $\underline{\phi}_n$:

$$\underline{u}(t) = q_1(t)\underline{\phi}_1 + q_2(t)\underline{\phi}_2 + \ldots\ldots + q_N(t)\underline{\phi}_N \tag{3.23}$$

$q_n(t)$ in Eq. (3.23) are the modal amplitudes, or modal coordinates.

For a set of $\underline{\phi}_n$, we can determine q_n by employing the orthogonality property of modal vectors. Let's pre-multiply all terms in Eq. (3.22) by $\underline{\phi}_n^T \underline{m}$.

$$\underline{\phi}_n^T \underline{m}\, \underline{u} = q_1 \left(\underline{\phi}_n^T \underline{m}\, \underline{\phi}_1\right) + \cdots + q_n \left(\underline{\phi}_n^T \underline{m}\, \underline{\phi}_n\right) + \cdots + q_N \left(\underline{\phi}_n^T \underline{m}\, \underline{\phi}_N\right) \tag{3.24}$$

All parentheses terms are zero due to modal orthogonality with respect to mass, except the $\left(\underline{\phi}_n^T\ \underline{m}\ \underline{\phi}_n\right)$ term. Then,

$$q_n(t) = \frac{\underline{\phi}_n^T\ \underline{m}\ \underline{u}}{\underline{\phi}_n^T\ \underline{m}\ \underline{\phi}_n} \tag{3.25}$$

The denominator term is equal to 1 if the modes are mass normalized.

Example 3.5. Determine the modal expansion of $\underline{u} = \begin{Bmatrix}1\\1\end{Bmatrix}$ in terms of the modal vectors determined in Example 3.4.

$$q_1 = \underline{\phi}_1^T\ \underline{m}\ \underline{u} = \{0.526 \quad 0.851\}\begin{bmatrix}1 & 0\\0 & 1\end{bmatrix}\begin{Bmatrix}1\\1\end{Bmatrix} = 1.377$$

$$q_2 = \underline{\phi}_2^T\ \underline{m}\ \underline{u} = 0.325$$

Substituting into Eq. (3.23),

$$\underline{u} = 1.377\begin{Bmatrix}0.526\\0.851\end{Bmatrix} + 0325\begin{Bmatrix}0.851\\-0.526\end{Bmatrix} = \begin{Bmatrix}1.0\\1.0\end{Bmatrix}$$

3.4 FORCED VIBRATION UNDER EARTHQUAKE EXCITATION

We will reconsider the equation of motion of a MDOF system that was given by Eq. (3.3).

$$\underline{m}\ \underline{\ddot{u}} + \underline{c}\ \underline{\dot{u}} + \underline{k}\ \underline{u} = \underline{m}\ \underline{l}\ \ddot{u}_g(t) \tag{3.3}$$

u can be expanded in terms of modal vectors by using Eq. (3.23).

$$\underline{u}(t) = \sum_{r=1}^{N} \underline{\phi}_r\ q_r(t) \tag{3.26}$$

Substituting $u(t)$ from Eq. (3.26) into Eq. (3.3) and calculating the appropriate time derivatives in Eq. (3.3), we obtain

$$\sum_r \underline{m}\ \underline{\phi}_r\ \ddot{q}_r(t) + \sum_r \underline{c}\ \underline{\phi}_r\ \dot{q}_r(t) + \sum_r \underline{k}\ \underline{\phi}_r\ q_r(t) = -\underline{m}\ \underline{l}\ \ddot{u}_g \tag{3.27}$$

Pre-multiply each term in Eq. (3.27) by $\underline{\phi}_n^T$,

$$\sum_r \underline{\phi}_n^T \underline{m}\ \underline{\phi}_r\ \ddot{q}_r + \sum_r \underline{\phi}_n^T \underline{c}\ \underline{\phi}_r\ \dot{q}_r + \sum_r \underline{\phi}_n^T \underline{k}\ \underline{\phi}_r\ q_r = -\underline{\phi}_n^T \underline{m}\ \underline{l}\ \ddot{u}_g \tag{3.28}$$

Only those terms with $r=n$ are non-zero due to the orthogonality of modes. Although this is theoretically valid for $\underline{m}$ and $\underline{k}$, we can also assume the orthogonality of modal vectors with respect to $\underline{c}$.

$$\left(\underline{\phi}_n^T \underline{m}\ \underline{\phi}_n\right)\ddot{q}_n + \left(\underline{\phi}_n^T \underline{c}\ \underline{\phi}_n\right)\dot{q}_n + \left(\underline{\phi}_n^T \underline{k}\ \underline{\phi}_n\right)q_n = -\underline{\phi}_n^T \underline{m}\ \underline{l}\ \ddot{u}_g \tag{3.29}$$

The terms in the first, second and third parentheses on the left hand side are the modal mass M_n, modal damping C_n and modal stiffness K_n, respectively. The term $\underline{\phi}_n^T \underline{m}\ \underline{l}$ on the right hand side is called the modal excitation factor, L_n.

$$M_n = \underline{\phi}_n^T \underline{m}\ \underline{\phi}_n \tag{3.30}$$

$$C_n = \underline{\phi}_n^T \underline{c}\ \underline{\phi}_n \tag{3.31}$$

$$K_n = \underline{\phi}_n^T \underline{k}\ \underline{\phi}_n \tag{3.32}$$

$$L_n = \underline{\phi}_n^T \underline{m}\ \underline{l} \tag{3.33}$$

When the parentheses terms in Eq. (3.29) are replaced with the definitions in Eqs. (3.30) to (3.33), a compact form is obtained.

$$M_n\ \ddot{q}_n + C_n\ \dot{q}_n + K_n q_n = -L_n \ddot{u}_g \tag{3.34}$$

Dividing all terms by M_n and introducing the modal damping ratio and modal vibration frequency from Section **2.4.1** leads to a final normalized form.

$$\ddot{q}_n + 2\xi_n\ \omega_n\ \dot{q}_n + \omega_n^2\ q_n = -\frac{L_n}{M_n}\ \ddot{u}_g \tag{3.35}$$

Eq. (3.35) is valid for all modes, n = 1, 2… N. This is equivalent to a SDOF system in the modal coordinate q_n.

Equations (3.29-3.35) describe the *modal superposition procedure* where the system of N-coupled equations of motion of the MDOF system in Eq. (3.3) is replaced with N-

uncoupled equations of motion of equivalent SDOF systems in Eq. (3.35). This procedure provides significant advantages because working with coupled stiffness and mass matrices is much more difficult in applying numerical integration methods compared to integrating the uncoupled equations of motion separately.

Now, let's recall the equation of motion of a SDOF system under base excitation $\ddot{u}_g$ from Eq. (2.6). When Eq. (2.6) is normalized similar to the normalization of Eq. (3.34) into Eq. (3.35), we obtain

$$\ddot{u} + 2\xi_n \omega_n \dot{u} + \omega_n^2 u = -\ddot{u}_g \tag{3.36}$$

The only difference between Eq. (3.35) and Eq. (3.36) is the $\frac{L_n}{M_n}$ term applied to the ground excitation $\ddot{u}_g$ in the modal equation of motion. Therefore the solution procedures developed for SDOF systems under earthquake excitation in Chapter **2** are also valid for solving Eq. (3.35).

3.4.1 Modal Superposition

Modal superposition procedure for solving Eq. (3.3) is summarized below in a stepwise form.

1. Carry out eigenvalue analysis of Eq. (3.8) and determine the modal properties ($\underline{\phi}_n$, ω_n) for *n*=1, 2……N.
2. Construct Eq. (3.34) or (3.35) for each mode *n*.
3. Solve Eq. (3.34) by using the methods developed for SDOF systems in Chapter 2 ($\ddot{u}_g$ is scaled by $\frac{L_n}{M_n}$), and determine $q_n(t)$ for *n*=1, 2……N.
4. Transform from modal to physical coordinates by using Eq. (3.26).

3.4.2 Response Spectrum Analysis

The third step in the mode superposition analysis procedure above can also be performed by response spectrum analysis in a very simple manner. Let $S_d\ (T,\ \xi)$ be the displacement spectrum for $\ddot{u}_g(t)$. Then,

$$S_{dn} = S_d(T_n\ ,\xi_n) \tag{3.37}$$

and

$$q_{n,max} = \frac{L_n}{M_n} . S_{dn} \equiv \frac{L_n}{M_n} \frac{PSa_n}{\omega_n^2} \tag{3.38}$$

Also

$$\ddot{q}_{n,max} = \frac{L_n}{M_n} \; PSa_n \tag{3.39}$$

where

$$PSa_n = \; \omega_n^2 \, S_{dn} \tag{3.40}$$

Accordingly,

$$\underline{u}_{n,max} = \; \underline{\phi}_n \, q_{n,max} \equiv \underline{\phi}_n . \frac{L_n}{M_n} \, S_{dn} = \; \underline{\phi}_n \, \frac{L_n}{M_n} \, \frac{PSa_n}{\omega_n^2} \tag{3.41}$$

In Eq. (3.41) above, $\underline{u}_{n,max}$ is the maximum value of the *n*'th mode displacement vector $\underline{u}_n$. However since the time dependence is lost in Eq. (3.44), we cannot apply Eq. (3.26) directly and combine the maximum modal displacement for obtaining the maximum displacement distribution $\underline{u}_{max}$. Since all $q_{n,max}$ and accordingly $\underline{u}_{n,max}$ do not occur simultaneously,

$$\underline{u}_{max} \; \leq \; \underline{u}_{1,max} + \; \underline{u}_{2,max} + \; \ldots\ldots\ldots + \; \underline{u}_{\mathrm{N},max}$$

or

$$\begin{Bmatrix} u_1 \\ u_2 \\ \vdots \\ u_N \end{Bmatrix}_{max} \leq \begin{Bmatrix} u_{11} \\ u_{21} \\ \vdots \\ u_{N1} \end{Bmatrix}_{max} + \ldots . + \begin{Bmatrix} u_{N1} \\ u_{N2} \\ \vdots \\ u_{NN} \end{Bmatrix}_{max}$$

Modal responses are independent from each other, and the maximum values of a response parameter (displacement, rotation, internal force, moment, etc) occur at different times at each mode, without any synchronization. Hence a statistical combination is necessary for obtaining the maximum combined response. The SRSS (Square Root of the Sum of Squares) rule provides good approximation for combining the modal maxima of displacement components.

$$u_{1,max} = (u_{11,max}^2 + \; u_{21,max}^2 + \; \ldots . + u_{\mathrm{N}1,max}^2)^{\,1/2} \tag{3.42}$$

or, in general

$$u_{j,max} = (u_{1j,max}^2 + u_{2j,max}^2 + \ldots\ldots + u_{Nj,max}^2)^{1/2} \tag{3.43}$$

SRSS is equally applicable for estimating the maximum value of any force parameter (moment, shear, stress, etc.) or displacement parameter (curvature, rotation, displacement, strain, etc.) from the superposition of the associated maximum modal values.

Example 3.6. Determine the maximum displacement distribution of the 3-story shear frame in Fig. (a) under the acceleration spectrum given in Fig. (b). The results of eigenvalue analysis are also given below.

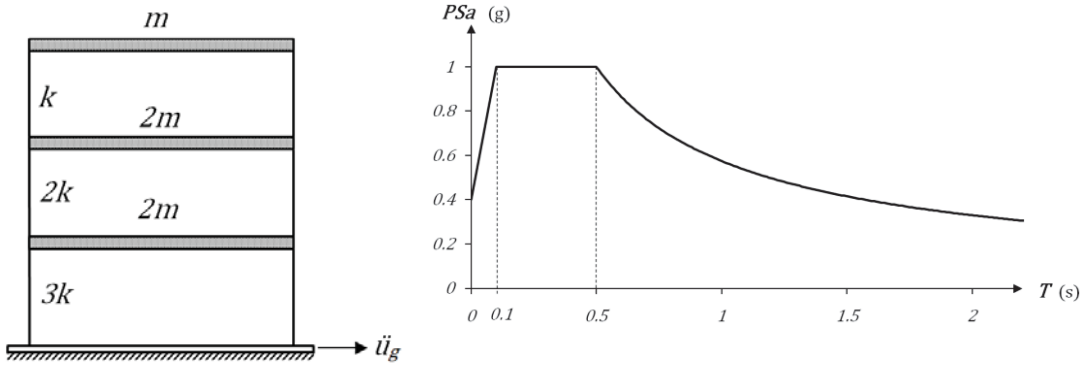

(a) (b)

$k = 140\,000\ kN/m$ $m = 175\,000\ kg$ k : total lateral stiffness for both columns

$$\underline{\phi}_1 = \begin{Bmatrix} 0.314 \\ 0.686 \\ 1.00 \end{Bmatrix} \quad \underline{\phi}_2 = \begin{Bmatrix} -0.50 \\ -0.50 \\ 1.00 \end{Bmatrix} \quad \underline{\phi}_3 = \begin{Bmatrix} 1.00 \\ -0.686 \\ 0.313 \end{Bmatrix}$$

$$\omega_1 = 15.84\ r/s \quad \omega_2 = 34.64\ r/s \quad \omega_3 = 50.50\ r/s$$

$$T_1 = 0.40\ s \quad T_2 = 0.18\ s \quad T_3 = 0.125\ s$$

Solution

When we enter the response spectrum with the modal period values, we determine the modal spectral acceleration values.

$$Sa_1 = Sa_2 = Sa_3 = 1.0\ g$$

Then the modal masses and modal excitation factors are determined.

$$M_1 = \underline{\phi}_1^T\, \underline{m}\, \underline{\phi}_1 = 374\,700\ kg \quad M_2 = 350\,000\ kg \quad M_3 = 531\,000\ kg$$
$$L_1 = \underline{\phi}_1^T\, \underline{m}\, \underline{1} = 525\,350\ kg \quad L_2 = -175\,000\ kg \quad L_3 = 165\,550\ kg$$

$$\frac{L_1}{M_1} = 1.40 \quad \frac{L_2}{M_2} = -0.50 \quad \frac{L_3}{M_3} = 0.31$$

Let $q_{n,max} = q_n$ (drop the *max* index). q_n are obtained from Eq. (3.38) and maximum modal displacements are determined from Eq. (3.41).

$$q_1 = \frac{L_1}{M_1}\frac{Sa_1}{\omega_1^2} = 5.47\ cm \quad q_2 = -0.41\ cm \quad q_3 = 0.12\ cm$$

$$\underline{u}_1 = \underline{\phi}_1\, q_1 = \begin{Bmatrix}1.72\\3.76\\5.47\end{Bmatrix}_{cm} \quad \underline{u}_2 = \begin{Bmatrix}-0.20\\-0.20\\0.41\end{Bmatrix}_{cm} \quad \underline{u}_3 = \begin{Bmatrix}0.12\\-0.10\\0.04\end{Bmatrix}_{cm}$$

Finally, the modal spectral displacements are combined with the SRSS rule for obtaining the maximum story displacement distribution.

$$\underline{u} = \begin{Bmatrix}\sqrt{1.72^2 + (-0.20)^2 + (0.12)^2} = 1.74\\ \sqrt{3.76^2 + (-0.20)^2 + (-0.10)^2} = 3.77\\ \sqrt{5.47^2 + 0.41^2 + 0.04^2} = 5.50\end{Bmatrix}_{cm}$$

It may be noted that $\underline{u} \approx \underline{u}_1$, i.e. the first mode displacements dominate the total displacement distribution. In particular,

$$u_{roof} \simeq \sqrt{5.47^2 + 0.41^2 + 0.04^2} = 5.50 \text{ cm}$$

3.4.3 Equivalent Static (Effective) Modal Forces

We can define an equivalent static force vector $\underline{f}_n(t)$ for each mode n, which produces the modal spectral displacements $\underline{u}_n(t)$ when they are applied to the MDOF system.

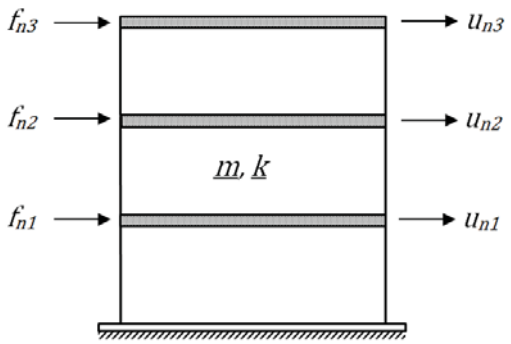

At any time t during dynamic response, dynamic equilibrium requires

$$\boxed{\underline{f}_n(t) = \underline{k}\,\underline{u}_n(t)} \tag{3.45}$$

Substituting $\boxed{\underline{u}_n(t) = \underline{\phi}_n\, q_n(t)}$ from Eq. (3.10) into Eq. (3.11),

$$\underline{f}_n(t) = \underline{k}\,\underline{\phi}_n q_n(t) = \underline{k}\,\underline{u}_n(t) \tag{3.46}$$

We can express the modal forces in a simpler form. Eq (3.14) for free vibration can be written as

$$\underline{k}\,\underline{\phi}_n = \omega_n^2\,\underline{m}\,\underline{\phi}_n \tag{3.47}$$

Multiplying each term by q_n gives

$$\underline{k}\,\underline{\phi}_n q_n = \omega_n^2\,\underline{m}\,\underline{\phi}_n q_n \tag{3.48}$$

Substituting the right hand side of Eq. (3.48) for the middle term in Eq. (3.46), we obtain

$$\underline{f}_n(t) = \omega_n^2\,\underline{m}\,\underline{\phi}_n q_n(t) \tag{3.49}$$

This is a more practical expression since the diagonal matrix $\underline{m}$ is easier to work with compared to the banded matrix $\underline{k}$ having off-diagonal terms.

If we employ response spectrum analysis, then $q_n(t) = q_{n,\max}$ in Eq. (3.49). Then, substituting $q_{n,\max}$ from Eq. (3.38) into Eq. (3.49),

$$\underline{f}_n = \omega_n^2\,\underline{m}\,\underline{\phi}_n\left[\frac{L_n}{M_n}\frac{S_{an}}{\omega_n^2}\right] \tag{3.50}$$

Sa=w^2 Sd

Finally, we obtain a simplified expression for the modal spectral force vector after rearranging Eq. (3.50).

$$\underline{f}_n = \frac{L_n}{M_n}\left(\underline{m}\,\underline{\phi}_n\right) S_{an} \tag{3.51}$$

The total force at the base V_{bn} (modal base shear force) is equal to $\underline{1}^T\underline{f}_n$ where $\underline{1}$ is the unit vector.

$$V_{bn} = \underline{1}^T\,\underline{f}_n = \frac{L_n}{M_n}\left(\underline{1}^T\,\underline{m}\,\underline{\phi}_n\right) S_{an} \equiv \frac{L_n}{M_n}\left(\underline{\phi}_n^T\underline{m}\,\underline{1}\right) S_{an} \tag{3.52}$$

Then,

$$V_{bn} = \frac{L_n^2}{M_n}\,S_{an} \equiv M_n^*\,S_{an} \tag{3.53}$$

where $M_n^* = \frac{L_n^2}{M_n}$ is the *effective modal mass*. With this definition, the spectral response at each mode under an earthquake base excitation that is expressed by its acceleration response

spectrum can be represented on a simple sketch of an equivalent SDOF system as shown in Fig. (3.3).

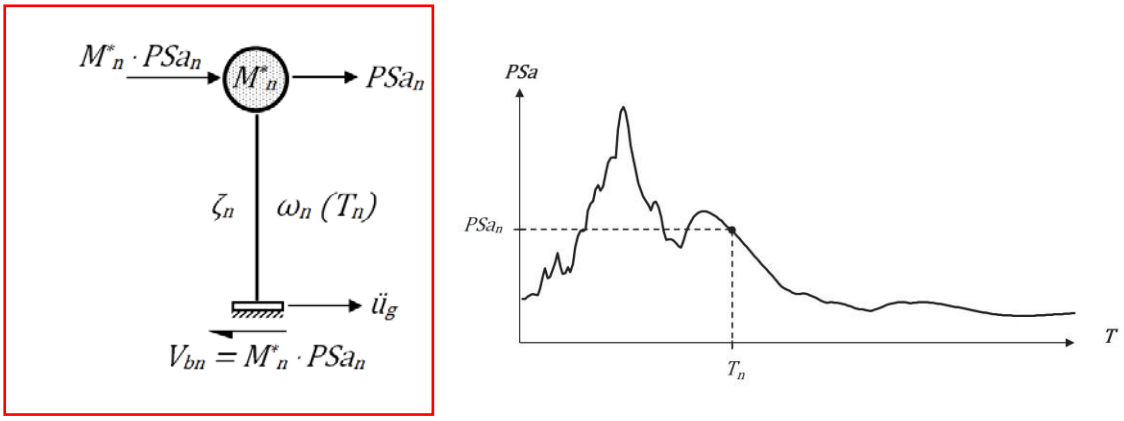

Fig. 3.3. SDOF representation of spectral modal response at mode *n*.

Effective modal mass has an important practical aspect such that the sum of effective modal masses for all modes is equal to the total mass of the building system.

$$\sum_{n}^{modes} M_n^* = \sum_{i}^{stories} m_i \tag{3.54}$$

This is exact for a shear frame, and quite accurate for an actual building structure. Effective modal mass can be directly calculated from the mass matrix and the *n*'th mode vector.

$$M_n^* = \frac{\left(\underline{\phi}_n^T\, \underline{m}\, \underline{1}\right)^2}{\underline{\phi}_n^T\, \underline{m}\, \underline{\phi}_n} \tag{3.55}$$

Example 3.7. Calculate the modal force vectors for the frame in Example 3.6. Also calculate the effective modal masses, modal base shear forces, and modal moments at the top end of the first story columns. Combine these forces and moments by SRSS for calculating the total base shear force and first story column top moment.

Modal Forces

$$\underline{f}_1 = \frac{L_1}{M_1}\left(\underline{m}\,\underline{\phi}_1\right) Sa_1 = 1.40 \begin{bmatrix} 2m & 0 & 0 \\ 0 & 2m & 0 \\ 0 & 0 & m \end{bmatrix} \begin{Bmatrix} 0.314 \\ 0.687 \\ 1.00 \end{Bmatrix} . g$$

$$\underline{f_1} = \begin{Bmatrix} 1\,509 \\ 3\,302 \\ 2\,408 \end{Bmatrix}_{kN} \quad \underline{f_2} = \begin{Bmatrix} -858 \\ -858 \\ 858 \end{Bmatrix}_{kN} \quad \underline{f_3} = \begin{Bmatrix} 1\,064 \\ -728 \\ 167 \end{Bmatrix}_{kN}$$

Effective modal masses

From Eq. (3.55),

$M_1^* = 736{,}550$ kg $(84.2\%\, M)$ $\quad M_2^* = 87{,}500$ kg $(10\%\, M)$ $\quad M_3^* = 51{,}275$ kg $(5.8\%\, M)$

$$M_1^* + M_2^* + M_3^* \simeq 875\,000\ kg \ \ (100\%\, M\,)$$

M is the total mass where *M*=5*m*=5x175,000 kg=875,000 kg. Therefore the sum of effective modal masses is equal to the total mass (inaccuracy is due to the decimal truncation in modal vectors).

Modal base shear forces

$$V_{bn} = M_n^*\, Sa_n$$

$$V_{b1} = 736{,}550\ kg\ X\ 9.81\ \frac{m}{s^2} = 7226\ kN\ ;\ \ V_{b2} = -858\ kN\ ;\ \ V_{b3} = 503\ kN$$

Note that $V_{bn} = \sum_{j=1}^{3} f_{nj}$ for all *n* =1-3.

$$V_b \simeq \sqrt{V_{b1}^2 + V_{b2}^2 + V_{b3}^2} = 7294\ kN$$

Modal column moments

$M^{top} = \frac{1}{2}\, V\, h$ where *V* is the shear force in the column and *h* is the story height. $V = \frac{1}{2}\, V_b$ at the first story columns. Then the modal column top moments at the first story are;

$$M_1^{top} = \frac{1}{2}\left(\frac{1}{2} \cdot 7226\right) h = 1806\, h\ ;\ \ M_2^{top} = 214.5\, h\ \ ;\ \ \ M_3^{top} = 126\, h$$

$$M^{top} \simeq \sqrt{(M_1^{top})^2 + (M_2^{top})^2 + (M_3^{top})^2} = 1823\, h\ (kN \cdot m)$$

Example 3.8. Consider the frame given in Example 3.2. If the frame is subjected to the ground excitation defined by the acceleration spectrum given in Example 3.6, determine the displacement of the mass at end B, the base shear force and base moment at the support, and the top moment of the column. Let *EI*=4000 kN-m^2, *m*=4 tons and *h*=4 m.

Solution

$T_n = 2\pi/\omega_n$, which gives $T_1 = 1.786$ s and $T_2 = 0.407$ s from the results of Example 3.2. The corresponding spectral accelerations can be determined from the acceleration response spectrum of Example 3.6, as $S_{a1} = 0.34$ g and $S_{a2} = 1.0$ g.

$$\begin{aligned} M_n &= \underline{\phi}_n^T\, \underline{m}\, \underline{\phi}_n \quad ; \quad M_1 = 17.99 \text{ tons} \qquad M_2 = 5.145 \text{ tons} \\ L_n &= \underline{\phi}_n^T\, \underline{m}\, \underline{1} \quad ; \quad L_1 = -3.48 \text{ tons} \qquad L_2 = 6.14 \text{ tons} \end{aligned} \tag{1}$$

$$\frac{L_1}{M_1} = -0.193 \quad \frac{L_2}{M_2} = 1.193$$

Modal amplitudes

$$q_n = \frac{L_n}{M_n}\frac{Sa_n}{\omega_n^2} \quad ; \quad q_1 = -0.0522 \text{ m} \qquad q_2 = 0.0492 \text{ m} \tag{2}$$

Modal displacement vectors

$$\underline{u}_n = \underline{\phi}_n\, q_n \quad ; \quad \underline{u}_1 = \begin{Bmatrix} -0.0522 \\ 0.0976 \end{Bmatrix}_{\text{m}} \quad \underline{u}_2 = \begin{Bmatrix} 0.0492 \\ 0.0263 \end{Bmatrix}_{\text{m}} \tag{3}$$

where

$$\underline{u}_n = \begin{Bmatrix} u_{Bn} \\ v_{Bn} \end{Bmatrix} ; \quad n = 1, 2$$

Displacements at the B end (SRSS combination)

$$u_B = \sqrt{(-0.0522)^2 + (0.0492)^2} = 0.0717 \text{ m} \quad \text{(Both modes contribute)}$$

$$v_B = \sqrt{(0.0976)^2 + (0.0263)^2} = 0.1011 \text{ m} \qquad \text{(1'st mode dominant)}$$

Internal forces in column OA

Let's denote the bottom end (fixed end) of the column by O. The end forces (lateral force and bending moment) of column OA can be determined both by the stiffness analysis of the column by using the modal end displacements, or by applying the equivalent static modal forces and calculating the associated modal internal forces. We will do both.

a) Stiffness analysis: Let's write the stiffness equation for column OA at the *n*'th mode.

$$\begin{Bmatrix} F_O \\ M_O \\ F_A \\ M_A \end{Bmatrix}_n = \frac{EI}{h} \begin{bmatrix} \frac{12}{h^2} & -\frac{6}{h} & -\frac{12}{h^2} & -\frac{6}{h} \\ -\frac{6}{h} & 4 & \frac{6}{h} & 2 \\ -\frac{12}{h^2} & \frac{6}{h} & \frac{12}{h^2} & \frac{6}{h} \\ -\frac{6}{h} & 2 & \frac{6}{h} & 4 \end{bmatrix} \begin{Bmatrix} u_O \\ \theta_O \\ u_A \\ \theta_A \end{Bmatrix}_n \tag{4}$$

Note that $u_O = \theta_O = 0$ (fixed end), $u_A = u_B$ and $\theta_B = {}^{v_B}/_{h}$. Inserting the associated modal displacements from Eq. (3), together with *EI* and *h* values into Eq. (4),

$$\begin{Bmatrix} F_O \\ M_O \\ F_A \\ M_A \end{Bmatrix}_1 = \begin{Bmatrix} 2.55 \ \text{kN} \\ -29.5 \ \text{kN.m} \\ -2.55 \ \text{kN} \\ 19.3 \ \text{kN.m} \end{Bmatrix} \quad \text{and} \quad \begin{Bmatrix} F_O \\ M_O \\ F_A \\ M_A \end{Bmatrix}_2 = \begin{Bmatrix} -46.76 \ \text{kN} \\ 86.95 \ \text{kN.m} \\ 46.76 \ \text{kN} \\ 100.1 \ \text{kN.m} \end{Bmatrix}$$

Base shear force and base moment at O, and moment at A (SRSS combination)

$$V_b = \sqrt{(2.55)^2 + (46.76)^2} = 46.83 \text{ kN} \qquad \text{(2'nd mode dominant)}$$

$$M_b = \sqrt{(29.5)^2 + (86.95)^2} = 91.82 \text{ kN.m} \qquad \text{(2'nd mode dominant)}$$

$$M_A = \sqrt{(19.3)^2 + (100.1)^2} = 101.94 \text{ kN.m} \qquad \text{(2'nd mode dominant)}$$

b) Equivalent static modal forces: From Eq. (3.51),

$$\underline{f_n} = \frac{L_n}{M_n}\left(\underline{m}\,\underline{\phi_n}\right).S_{an} \quad ; \quad \underline{f_1} = \begin{Bmatrix} -2.57 \\ 4.81 \end{Bmatrix}_{\text{kN}} \quad \text{and} \quad \underline{f_2} = \begin{Bmatrix} 46.81 \\ 25.04 \end{Bmatrix}_{\text{kN}}$$

The modal forces and the associated modal moment diagrams of the column OA are shown on the frame below.

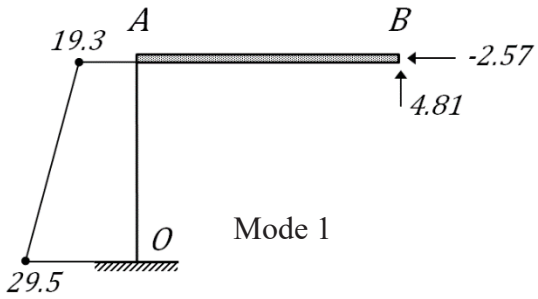

Mode 1

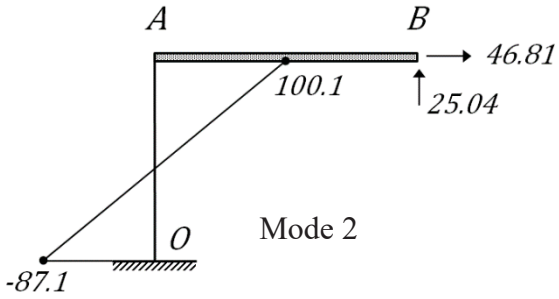

Mode 2

Modal base shear forces, base moments and moments at A can be calculated from statics. Then their SRSS combinations give the final values.

$$V_{b1} = -2.57, \qquad V_{b2} = 46.81\,, \qquad V_b = \sqrt{(2.57)^2 + (46.81)^2} = 46.88 \ \text{kN}$$

$$M_{b1} = 29.5, \qquad M_{b2} = -87.08\,, \qquad M_b = \sqrt{(29.5)^2 + (87.08)^2} = 91.94 \ \text{kN.m}$$

$$M_{A1} = 19.3, \qquad M_{A2} = 100.1\,, \qquad M_A = \sqrt{(19.3)^2 + (100.1)^2} = 102.04 \ \text{kN.m}$$

These values are very close to the values calculated from stiffness analysis. The differences are due to truncation errors.